HIGHWAY RESEARCH RECORD

Number 431

Soil Mechanics: Design

6 reports
prepared for the
52nd Annual Meeting

Subject Areas

62 Foundations (Soils)
63 Mechanics (Earth Mass)
64 Soil Science

HIGHWAY RESEARCH BOARD
DIVISION OF ENGINEERING NATIONAL RESEARCH COUNCIL
NATIONAL ACADEMY OF SCIENCES—NATIONAL ACADEMY OF ENGINEERING
Washington, D.C. 1973

NOTICE

The studies reported herein were not undertaken under the aegis of the National Academy of Sciences or the National Research Council. The papers report research work of the authors that was done at the institutions named by the authors. The papers were offered to the Highway Research Board of the National Research Council for publication and are published here in the interest of the dissemination of information from research, one of the major functions of the Highway Research Board.

Before publication, each paper was reviewed by members of the HRB committee named as its sponsor and accepted as objective, useful, and suitable for publication by the National Research Council. The members of the review committee were chosen for recognized scholarly competence and with due consideration for the balance of disciplines appropriate to the subject concerned.

Responsibility for the publication of these reports rests with the sponsoring committee. However, the opinions and conclusions expressed in the reports are those of the individual authors and not necessarily those of the sponsoring committee, the Highway Research Board, or the National Research Council.

Each report is reviewed and processed according to the procedures established and monitored by the Report Review Committee of the National Academy of Sciences. Distribution of the report is approved by the President of the Academy upon satisfactory completion of the review process.

ISBN 0-309-02161-8
Library of Congress Catalog Card No. 73-8342
Price: $2.20
Available from
Highway Research Board
National Academy of Sciences
2101 Constitution Avenue, N.W.
Washington, D.C. 20418

CONTENTS

FOREWORD

This RECORD covers aspects of pavement design relating to the contributions of various supporting layers in the pavement system. It will be of interest to pavement design engineers and soils engineers.

The national interest in conservation of resources gives added emphasis to the work of Hadley, Hudson, and Kennedy in developing a structural design procedure for including stabilized layers in the pavement system. The design system handles stabilized layers supporting either portland cement concrete or asphaltic concrete pavements.

Scrivner, Michalak, and Moore present a method for calculating the elastic modulus of the pavement layer, defined to be the base and surfacing, and for the subgrade layer from data obtained by a measurement of surface deflection. These moduli are used in the solution of typical pavement design problems. The computer program developed to perform the calculations can be incorporated into a comprehensive flexible pavement design system.

A characterization of subgrade soils for pavements, to be constructed in areas subjected to freezing and thawing, is reported on by Bergan and Monismith.

Brown has developed a chart from which Young's modulus for a bituminous layer may be determined in relation to known vehicle speed, temperature, loading time, and layer thickness.

A graphical technique for determining the elastic moduli of a two-layered structure from measured surface deflections is presented by Swift.

The permeability of granular materials was determined by use of a plastic device as described by Bowles.

STRUCTURAL DESIGN PROCEDURE FOR STABILIZED PAVEMENT LAYERS

William O. Hadley, Department of Civil Engineering,
Louisiana Technical University; and
W. Ronald Hudson and Thomas W. Kennedy, Center for Highway Research,
University of Texas at Austin

A design procedure is presented that can be used as an aid in the structural design of stabilized pavement layers. The system is based primarily on the prevention of tensile failures in the surface and base layers of a three-layer pavement structure and can be applied to take full advantage of those highway materials that possess cohesion or tensile strength. The design method consists of a series of design equations based on linear elastic layered theory, which can be used for computing tensile stresses and strains in the surface layer, tensile stresses and strains in the base layer, and compressive strains in the subgrade. Separate equations are presented for use in the design of high-modulus portland cement concrete pavements and for the design of flexible pavements and low-modulus portland cement concrete pavements. Procedures for proper application of the design equations are presented and include methods for selection of a critical design thickness. Characterization techniques are also provided for estimating limiting design stress criteria for the materials proposed for the various pavement layers. In addition, minimum design strain criteria are recommended for various cohesive highway materials.

•THE widespread use of pavements having stabilized pavement layers has created interest in development of procedures for the effective use of these pavement types. In particular there is need for a structural design method that is based on fundamental considerations and that emphasizes the contribution of stabilized layers to the behavior of the total pavement structure.

This paper presents a structural design procedure for the stabilized layers in a pavement structure, which is based on tensile resistance to a large number of applications of vehicle loads. The system is applicable to the design of cohesive pavements, i.e., those that have tensile strength.

DESIGN APPROACH

The formalized design system (1, 2) is shown in Figure 1 and is broken down into three phases. The first phase is concerned with characterization of the highway materials in the laboratory and requires techniques for estimating fundamental material properties, including modulus of elasticity, tensile strength, and tensile strain for all highway materials.

The second phase involves special material characterization techniques for considering the effects of temperature and loading rate on the properties of asphaltic materials to provide flexibility in the design. The other special consideration involves the establishment of minimum allowable stress and strain values (based on repeated loading studies) for each of the highway materials.

Sponsored by Committee on Strength and Deformation Characteristics of Pavement Sections.

The culmination of the design process occurs in the third phase where the minimum design criteria established in the second phase are used with design equations to obtain the required layer thickness. Because the thickness requirement of a stabilized layer can be affected by changes in the material properties of the layers, the design process can produce a large number of adequate design sections from which to choose. Economic analyses can then be used in the selection of the final design section.

SELECTION OF PAVEMENT THEORY

Layered theory has been used extensively since its development by Burmister in 1943; however, limited work has been done to incorporate the theory into a comprehensive structural design system. The design system presented here is based on a practical interpretation of layered theory, which emphasizes the contribution of each individual pavement layer to the behavior of the total pavement structure.

The hypothetical pavement design section adopted for this design system (Fig. 2) consists of three layers: a surface course, a base course (the stabilized layer underneath the surface layer is designated as the base layer regardless of pavement type), and the subgrade. The pavement is assumed to be loaded by two 4,500-lb loads uniformly distributed over circular areas and located 12 in. apart, center to center. This loading represents the present single-axle legal load limit of 18,000 lb.

The materials in each of the layers are assumed to be homogeneous, isotropic, and elastic. The surface and base layers are assumed to be infinite in extent in the lateral direction but of finite depth, whereas the subgrade layer is assumed to be infinite in both the horizontal and vertical directions. In addition, the continuity conditions require that there be continuous contact between the surface and base layers and between the base and subgrade layers.

DEVELOPMENT OF DESIGN EQUATIONS

Because layered theory provides a deterministic model for predicting stresses, strains, and deflections in a given pavement system, it has direct application to evaluation of existing pavement sections. The inputs required in the theory, i.e., number and thickness of layers, moduli, and Poisson's ratio, can be estimated for existing pavement materials.

On the other hand, layered theory cannot be used directly for the structural design of the individual layers of a pavement because the thicknesses of the layers are required as input for the theory. Iterative solutions of layered theory equations for variation in the pavement section could be used in the design process; however, this technique could require a large number of computer solutions and would be feasible for only the simplest of design problems. The greatest value of layered theory in design of pavement structures appears to be its use in development of design equations relating stresses and strains to the important variables in the design section, i.e., layer thickness and modulus of elasticity. These equations can then be used to obtain directly the combination of layer thickness and modulus of elasticity corresponding to a specified critical design stress or strain.

Mathematical models were developed for this design system by approximating the layered theory results with polynomial mathematical equations that included all of the important variables of the design section. Regression analysis techniques were used to develop the approximate models from a series of solutions obtained from the Chevron STRESS-N computer program (3) for various levels of the design variables. A stepwise regression technique was used to relate specific stresses and strains obtained from the Chevron STRESS-N computer program to the design variables.

TECHNIQUE OF DEVELOPING DESIGN EQUATIONS

The variables considered in the development of the design equations were modulus of elasticity, E_s; thickness of surface layer, T_s; modulus of elasticity, E_b; thickness of base layer, T_b; and modulus of elasticity of the subgrade, E_g. The ranges in these variables, which were used in the development of the design equations, are shown in

Figure 2. The values of modulus of elasticity in the surface layer provided for evaluation of low-modulus as well as high-modulus layers, whereas the range of modulus values for the base layer spanned the range expected for lime-treated, asphalt-treated, and cement-treated materials. The thicknesses selected were considered to be representative of those normally used in highway pavements.

Regression techniques were used to obtain equations for tensile stresses and strains in the bottom fibers of the upper two layers and vertical strain in the top of the subgrade in terms of the moduli and thicknesses of the pavement layers. The general form of the equation is $\log_{10}(Y) = f(X_1, X_2, \ldots X_n)$, where $\log_{10}(Y)$ is the logarithm of the dependent variable Y (i.e., stress or strain in a particular layer), and $X_1, X_2, X_3, \ldots X_n$ are the independent variables under consideration (i.e., layer moduli and thicknesses).

Separate equations were obtained for low- and high-modulus layers to provide flexibility in the type of highway pavement to be designed. The equations for low-modulus layers can be used for design of flexible pavements as well as for design of low-modulus portland cement concrete pavements, whereas the equations for high-modulus layers can be used for design of high-strength portland cement concrete pavements.

Design Equations for High-Modulus Surface Layers

The regression equations for pavement structures with surface layers exhibiting modulus-of-elasticity values in the range of 3.5×10^6 psi to 6.50×10^6 psi are given in this section. The pertinent statistical information concerning the equations is given in Table 1. The predictive capability of the equations is indicated by the standard errors of estimate, $\hat{S}_r$. Consequently, the tensile stress and strain in the base layer and compressive strain in the subgrade can be predicted within closer limits than can the tensile stress and strain in the surface layer. All five equations, however, provide adequate approximation to layered theory[1].

1. Tensile stress in bottom of base layer, σ_b:

$$\begin{aligned}\text{Log}_{10}(\sigma_b) \times 10^3 = [&1{,}333.84 + 46.868\,(E_b - 5.5) - 23.774\,(T_b - 7.5) \\ &-3.3610\,(E_b - 5.5)\,(T_b - 7.5) - 11.008\,(E_b - 5.5)^2 \\ &+1.6306\,(E_b - 5.5)^3 + 4.3026\,(T_s - 7.5)\,(T_b - 7.5) \\ &-39.310\,(E_s - 5.0) - 21.572\,(E_g - 8.0) + 1.7254\,(E_g - 8.0)^2 \\ &-80.972\,(T_s - 7.5) + 4.0607\,(E_b - 5.5)\,(T_s - 7.5) \\ &+3.4019\,(T_s - 7.5)^2] \end{aligned} \quad (1)$$

2. Tensile strain in bottom of base layer, ϵ_b:

$$\begin{aligned}\text{Log}_{10}(\epsilon_b) \times 10^3 = [&1{,}412.12 - 34.516\,(E_b - 5.5) - 19.891\,(T_b - 7.5) \\ &-3.3677\,(E_b - 5.5)\,(T_b - 7.5) + 2.0650\,(E_b - 5.5)^2 \\ &+3.9519\,(T_s - 7.5)\,(T_b - 7.5) - 37.103\,(E_s - 5.0) \\ &-21.293\,(E_g - 8.0) + 1.7920\,(E_g - 8.0)^2 - 76.216\,(T_s - 7.5) \\ &+3.9517\,(E_b - 5.5)\,(T_s - 7.5) + 2.7973\,(T_s - 7.5)^2] \end{aligned} \quad (2)$$

3. Compressive strain in subgrade, ϵ_c:

$$\begin{aligned}\text{Log}_{10}(\epsilon_c) \times 10^3 = [&1{,}744.52 - 34.206\,(E_b - 5.5) - 17.860\,(T_b - 7.5) \\ &-3.3359\,(E_b - 5.5)\,(T_b - 7.5) + 2.09191\,(E_b - 5.5)^2 \\ &-74.426\,(T_s - 7.5) + 4.1675\,(T_s - 7.5)\,(T_b - 7.5)\end{aligned}$$

[1]The original manuscript of this paper contained an appendix, Comparisons Between Design Equations and Layered Theory Equations. This appendix is available in Xerox form at cost of reproduction and handling from the Highway Research Board. When ordering, refer to XS-45, Highway Research Record 431.

$$+3.1465\ (T_s - 7.5)^2 - .44062\ (T_s - 7.5)^2\ (T_b - 7.5)$$
$$+3.9401\ (E_b - 5.5)\ (T_s - 7.5) - .44431\ (E_b - 5.5)^2\ (T_s - 7.5)$$
$$-11.482\ (E_s - 8.0) + 1.7026\ (E_s - 8.0)^2 - .16881\ (E_s - 8.0)^3$$
$$-38.520\ (E_s - 5.0) - 3.5104\ (E_s - 5.0)\ (T_s - 7.5)] \quad (3)$$

4. Tensile stress in bottom of surface layer, σ_s:

$$\text{Log}_{10}\ (\sigma_s + 26.4) \times 10^3 = [2{,}084.50 - 31.179\ (E_b - 5.5) - 37.176\ (T_b - 7.5)$$
$$-4.9726\ (E_b - 5.5)\ (T_b - 7.5) + 6.5353\ (T_s - 7.5)\ (T_b - 7.5)$$
$$-24.615\ (T_s - 7.5) - 1.2956\ (E_b - 5.5)\ (T_s - 7.5)^2$$
$$+8.2011\ (E_b - 5.5)\ (T_s - 7.5) - 9.3803\ (E_s - 5.0)\ (T_s - 7.5)$$
$$-7.2608\ (E_s - 8.0)] \quad (4)$$

5. Tensile strain in bottom of surface layer, ϵ_s:

$$\text{Log}_{10}\ (\epsilon_s + 5.15) \times 10^3 = [1{,}233.72 - 40.073\ (E_b - 5.5) - 35.042\ (T_b - 7.5)$$
$$-4.1767\ (E_b - 5.5)\ (T_b - 7.5) + 6.1426\ (T_s - 7.5)\ (T_b - 7.5)$$
$$-15.756\ (T_s - 7.5) + 7.0680\ (E_b - 5.5)\ (T_s - 7.5)$$
$$-8.1402\ (E_s - 8.0)] \quad (5)$$

Design Equations for Low-Modulus Surface Layers

The regression equations for pavement structures with surface layers exhibiting modulus-of-elasticity values in the range of 0.5 to 3.5 $\times$ 10^6 psi are given in this section. The pertinent statistical data concerning the equations are given in Table 2. From these results, it is obvious that the equation for tensile strain in surface layer ($R^2 = 0.100$) is not as adequate as the others in approximating layer theory equations; however, the equation can provide general design information at least through tensile strains of 50 micro-units. The predictive capability of the four other equations, as indicated by standard errors of estimate, $\hat{S}_r$, is adequate.

1. Tensile stress in bottom of base layer, σ_b:

$$\text{Log}_{10}\ (\sigma_b) \times 10^3 = [1{,}532.25 - 66.290\ (T_s - 7.5) - 35.264\ (T_b - 7.5)$$
$$+3.6935\ (T_s - 7.5)\ (T_b - 7.5) - 89.256\ (E_s - 2.0)$$
$$-8.3627\ (E_s - 2.0)\ (T_s - 7.5) + 44.289\ (E_b - 4.90)$$
$$-12.508\ (E_b - 4.90)^2 + 1.7468\ (E_b - 4.90)^3 + 2.9460\ (E_b - 4.90)$$
$$(T_s - 7.5) - 21.341\ (E_s - 8.0) + 1.7005\ (E_s - 8.0)^2] \quad (6)$$

2. Tensile strain in bottom of base layer, ϵ_b:

$$\text{Log}_{10}\ (\epsilon_b) \times 10^3 = [1{,}614.23 - 60.373\ (T_s - 7.5) - 30.108\ (T_b - 7.5)$$
$$+3.1786\ (T_s - 7.5)\ (T_b - 7.5) - 81.580\ (E_s - 2.0)$$
$$-8.9055\ (E_s - 2.0)\ (T_s - 7.5) - 50.011\ (E_b - 4.9)$$
$$+3.7758\ (E_b - 4.9)^2 + 2.7682\ (E_b - 4.9)\ (T_s - 7.5)$$
$$-21.619\ (E_s - 8.0) + 1.7407\ (E_s - 8.0)^2] \quad (7)$$

3. Compressive strain in subgrade, ϵ_c:

$$\text{Log}_{10}\ (\epsilon_c) \times 10^3 = [1{,}949.16 - 64.339\ (T_s - 7.5) - 33.750\ (T_b - 7.5)$$
$$+3.5397\ (T_s - 7.5)\ (T_b - 7.5) - 86.598\ (E_s - 2.0)$$
$$-8.4973\ (E_s - 2.0)\ (T_s - 7.5) - 49.905\ (E_b - 4.9)$$

Figure 1. System for structural design of stabilized pavement layers.

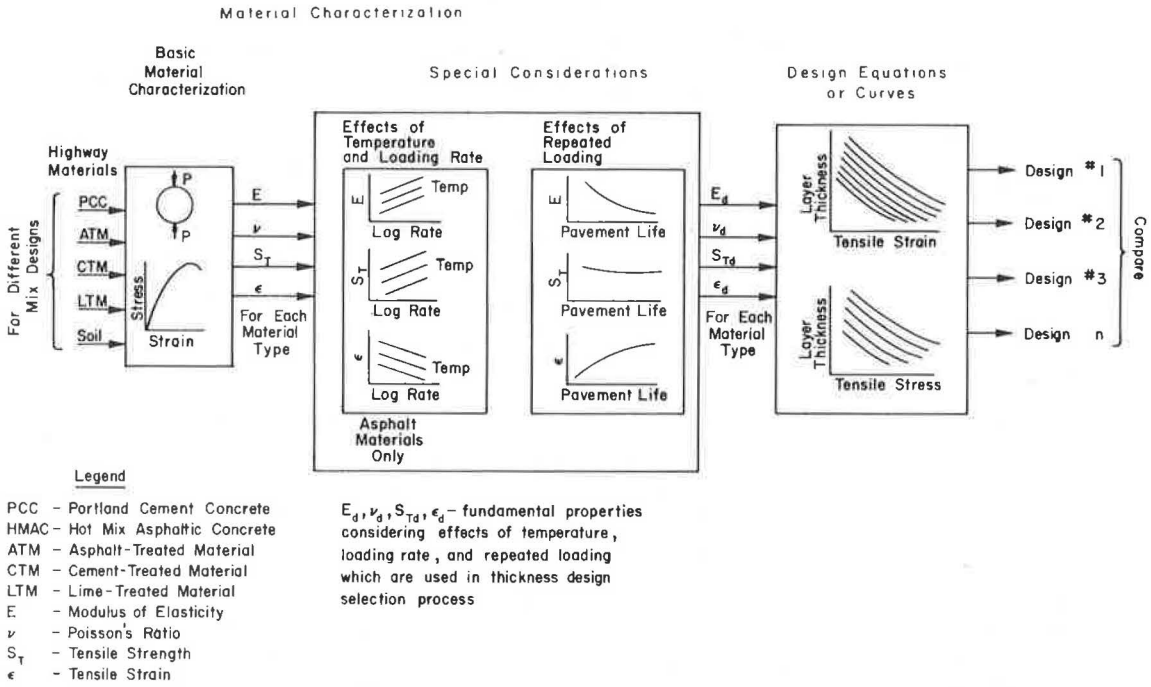

Figure 2. Hypothetical pavement section.

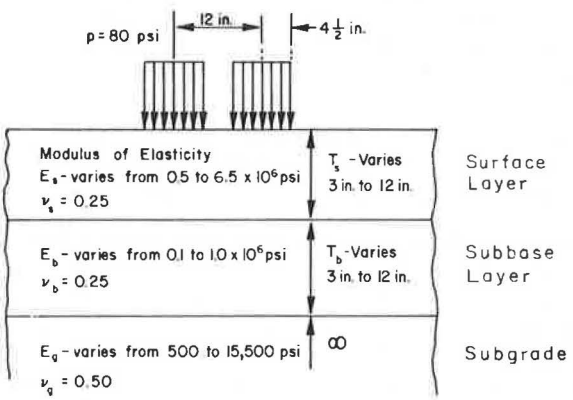

Table 1. Statistical data for regression equations: high-modulus surface layers.

Response Variable	Log Form	Coefficient of Determination	Standard Error of Estimate
Tensile stress in base layer	Log σ_b	0.989	±0.04635
Tensile strain in base layer	Log ϵ_b	0.983	±0.04388
Compressive strain in subgrade	Log ϵ_c	0.991	±0.03321
Tensile stress in surface layer	Log(σ_s + 26.4)	0.680	±0.18694
Tensile strain in surface layer	Log(ϵ_s + 5.15)	0.635	±0.1716

Table 2. Statistical data for regression equations: low-modulus surface layers.

Response Variable	Log Form	Coefficient of Determination	Standard Error of Estimate
Tensile stress in base layer	Log σ_b	0.969	±0.06649
Tensile strain in base layer	Log ϵ_b	0.964	±0.06212
Compressive strain in subgrade	Log ϵ_c	0.965	±0.06323
Tensile stress in surface layer	Log(σ_s + 55.0)	0.847	±0.10570
Tensile strain in surface layer	Log(ϵ_s + 56.4)	0.100	±0.40665

$$+3.7417\ (E_b - 4.9)^2 + 2.8438\ (E_b - 4.9)\ (T_s - 7.5)$$
$$-20.156\ (E_s - 8.0) + 1.6349\ (E_s - 8.0)^2] \quad (8)$$

4. Tensile stress function for surface layer, σ_s:

$$\text{Log}_{10}\ (\sigma_s + 55.0) \times 10^3 = [2{,}043.83 - 27.372\ (T_b - 7.5) - 4.3388\ (T_s - 7.5)^2$$
$$+3.66404\ (T_s - 7.5)\ (T_b - 7.5) + 126.90\ (E_s - 2.0)$$
$$-15.756\ (E_s - 2.0)\ (T_s - 7.5) - 35.357\ (E_s - 2.0)^2$$
$$-47.247\ (E_b - 4.90) + 3.9371\ (E_b - 4.90)^2$$
$$+6.6099\ (E_b - 4.9)\ (T_s - 7.5)] \quad (9)$$

5. Tensile strain function for surface layer, ϵ_s:

$$\text{Log}_{10}\ (\epsilon_s + 56.4) \times 10^3 = [1{,}845.4 - 13.892\ (T_b - 7.5) - 26.686\ (E_b - 4.90)$$
$$+14.129\ (E_s - 2.0)\ (E_b - 4.90)\ (T_s - 7.5)$$
$$+4.9443\ (E_b - 4.90)\ (T_s - 7.5)] \quad (10)$$

APPLICATION OF DESIGN EQUATIONS

The equations can be solved for any one of the variables so long as estimates of the others are available. Generally, the inputs for the equations would include a critical design stress or strain and modulus of elasticity for each of three pavement layers as well as an estimate of surface layer thickness. The resulting output from these solutions would then be the corresponding base design thickness. The equations can also be used to obtain the design thickness of the surface layer as well as the critical design tensile stress or strain for the upper two layers if proper estimates of the other variables are provided as inputs for the equations.

THICKNESS SELECTION PROCEDURE

The procedure for selecting a base thickness is shown in Figure 3 for a constant surface thickness and given material properties. The process is broken down into five separate designs. The first two design thicknesses are based on allowable tensile stress or strain in the base layer. The third design is based on compressive strain in the subgrade and is provided to ensure that lateral movement of the subgrade will not occur and that the integrity of the pavement system is maintained. The final two design thicknesses are obtained by checking to ensure that the tensile stresses and strains produced in the surface layer do not exceed the allowable values for the surface layer materials.

All five base thicknesses are compared in order to select a critical design thickness that will satisfy all conditions. A typical design analysis would involve a number of iterative computations because changes in types of material as well as different combinations of surface and base thicknesses can be evaluated in the process of selecting the most economical design section.

The equations presented in this paper are based on a pavement structure that includes a base layer with a modulus of elasticity in the range of 0.1×10^6 to 1×10^6 psi and cannot be used to evaluate the situation of a surface layer lying directly on the subgrade. Therefore, the fact that a base is not required for a given design stress or strain (i.e., $T_b = 0.0$) does not mean that a base is not required. Rather it indicates that a minimum thickness is adequate or that a lower quality material (i.e., one with a lower tensile strength) may be used for the particular design criteria.

MATERIAL CHARACTERIZATION

One of the more important aspects in the use of a theorectical design approach involves the estimation of the fundamental properties of the materials comprising the different stabilized pavement layers. Consequently the method of obtaining estimates of these properties is then an important link in the total design system.

BASIC CHARACTERIZATION

Because the design equations are based on linear elastic theory, it is necessary to characterize the pavement materials by the elastic constant of modulus of elasticity. It is equally important that estimates of design stresses and strains be obtained to ensure the proper selection of a critical design thickness. The method of obtaining estimates of these properties is then an important link in the design analysis. Because the method is based on tensile failures, material characterization by some type of tensile test is essential.

Recent developments in the use of the indirect tensile test have included a technique for estimating fundamental properties of modulus of elasticity, Poisson's ratio, tensile strength, and tensile failure strains (4, 5, 6) for different stabilized materials. This technique appears to be the most practical method available for obtaining estimates of fundamental material properties of cohesive highway materials. The test has been used to evaluate a wide variety of materials, including portland cement concrete and asphalt-treated materials (4, 18-25), lime-treated materials (26, 27, 28), and untreated cohesive soils (29, 30).

REPEATED LOADING CONSIDERATION

Because pavement failures have been attributed in some cases to fatigue of the pavement layers, the behavior of stabilized materials subjected to repeated applications of tensile stresses and strains is important in the design of the various pavement layers. In this design system (Fig. 1), the fatigue or repeated loading behavior of the various stabilized materials is used to establish the design stresses and strains that will ensure a longer fatigue life and thus a longer pavement life.

Design Tensile Stress

The design tensile stress is obtained by multiplying the tensile strengths of the materials to be used in the surface and base layers by an appropriate fatigue strength ratio. (Fatigue strength ratio of a material is defined here as the ratio of the fatigue strength of the material at 10^7 load applications to the ultimate strength of the material.) The following fatigue strength ratios were developed for a variety of materials from available fatigue studies:

Material	Fatigue Strength Ratio
Portland cement concrete	0.52
Soil cement; cement-treated materials	0.35
Lime-treated materials	0.35
Asphalt-treated materials	0.125

A lower bound on all test data for a particular study was used in this development (1, 2).

Design Tensile Strains

Most fatigue studies have been concerned primarily with an evaluation of fatigue strength; therefore, there is a definite lack of information concerning fatigue strain ratios, i.e., ratio of repeated applied strain to ultimate failure strain at some preselected number of load applications. Because information about fatigue strain ratios is unavailable, it was necessary to establish the following recommended allowable tensile strains based on available fatigue data (1, 2):

Material	Allowable Tensile Strain (micro-unit)
Portland cement concrete	20
Cement-treated materials	20
Lime-treated materials	20
Asphalt-treated materials	50

Compressive Strain in Subgrade

Information concerning the allowable compressive strain for subgrade materials is limited to that suggested by Dormon and Metcalf (34). Based on their recommendations, a critical design compressive strain of 420 micro-units, which corresponds to 10 million load applications, is accepted for use in this design subsystem.

EFFECTS OF TEMPERATURE AND RATE OF APPLICATION OF LOAD ON PROPERTIES OF ASPHALTIC MATERIALS

The use of asphalt-stabilized pavement layers creates a special problem for the design of a pavement section because material properties such as modulus of elasticity, Poisson's ratio, tensile strength, and tensile strain at failure are a function of both the rate of application of load and the temperature of the stabilized layer. Therefore, another important part of this design approach is a requirement for a technique with which to evaluate the effects of temperature and rate of loading on the properties of asphalt-stabilized mixtures. A characterization technique based on a study by Hudson and Kennedy (18) has been developed (1, 2, 35) and provides a method of estimating the temperature and rate dependence of asphaltic materials.

DESIGN APPLICATIONS

A design example is presented to illustrate the overall approach necessary in the structural design of a base. This problem illustrates the steps necessary in the design of an asphalt-stabilized base layer for a rigid pavement structure. The total design analysis included an evaluation of asphalt-stabilized base thickness requirements for summer and winter conditions as well as design considerations for two surface thicknesses and two portland cement concrete mixes.

The first step in the design process involves characterization of the materials used in the various pavement layers. The properties assumed for the portland cement concrete mixes and the asphalt-treated material are given in Table 3. The modulus of elasticity of the subgrade is assumed to be 8,000 psi, and the average ambient summer and winter temperatures are expected to be 85 F and 65 F respectively. The resulting estimates of material properties for the two design periods are also given in Table 3.

The second step involves determination of the design stress criteria for the various pavement layers. The design stress criteria are obtained from the product of the design tensile strength (Table 3) and the recommended fatigue strength ratios for the various pavement materials. The results of the procedure for obtaining the design stresses are given in Table 4. The design strain criteria used are those given previously.

The third step involves substitution of the various material properties, design criteria, and surface layer thickness in the design equations and solving for the base thicknesses that satisfy each of the five design criteria. The solutions to each of the eight individual designs evaluated in this example are given in Table 5.

The final step in the design process includes a comparison of the different design thicknesses and, with the aid of a set of decision criteria, the selection of a final base design thickness. For this example, only the eight different critical design thicknesses are compared. After the decision criteria are established, the final design could be selected from these eight critical base designs. From these results, it can be seen that, for this particular example problem, (a) an increase in surface layer thickness reduced the required base thickness and (b) the change in surface layer mix designs had very little effect on base requirements.

SUMMARY

In this paper a formalized design system, based on the prevention of tensile failures in pavement layers, has been presented for use in the structural design of stabilized pavement layers. Layered theory was selected as the basic design theory and was used in the development of a series of design equations relating tensile stresses and strains at selected locations in the pavement layers to a number of the more important design variables. Applications of the design equations to the structural design of stabilized

Figure 3. Process for selecting final base thickness.

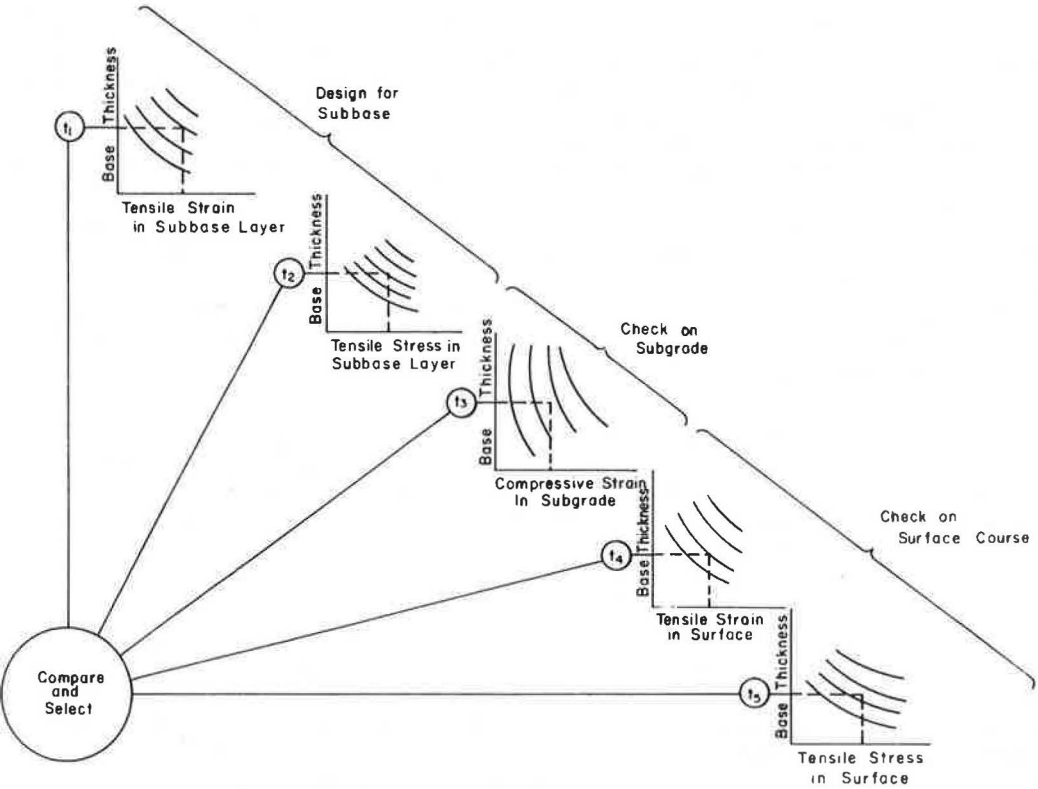

Table 3. Properties of portland cement concrete and asphalt-treated material.

Material	Measure
Portland cement concrete	
Mix 1	
Modulus of elasticity	4.75×10^6 psi
Tensile strength	310 psi
Mix 2	
Modulus of elasticity	3.50×10^6 psi
Tensile strength	270 psi
Asphalt-treated	
Summer conditions	
Modulus of elasticity	1.500×10^5 psi
Tensile strength	100 psi
Winter conditions	
Modulus of elasticity	3.50×10^5 psi
Tensile strength	180 psi
Subgrade (modulus of elasticity)	8.00×10^3 psi
Average summer temperature	85 F
Average winter temperature	65 F

Table 4. Determination of design criteria for use in design equations.

Material	Design Tensile Strength (psi)	Fatigue Strength Ratio	Design Stress[a] (psi)	Design Strain (micro-units)
Portland cement concrete				
Mix 1	310	0.52	160	20
Mix 2	270	0.52	140	20
Asphalt-treated				
Summer conditions	100	0.125	12.5	50
Winter conditions	180	0.125	22.5	50

[a]Design stress equals fatigue strength ratio times tensile strength.

Table 5. Base thickness requirements for design conditions.

Surface Layer Thickness (in.)	Mix Design	Modulus of Elasticity			Base Thickness for Design Criteria of				
		Surface (10^6 psi)	Base (10^5 psi)	Subgrade (10^3 psi)	σ_b	ϵ_b	ϵ_a	σ_s	ϵ_s
7.5	1	4.75	3.50(w)[a]	8.0	0	0	0	3.0	4.3
7.5	1	4.75	1.5(s)	8.0	0	0	0	4.0	7.1
8.5	1	4.75	3.5(w)	8.0	0	0	0	0	1.8
8.5	1	4.75	1.5(s)	8.0	0	0	0	0	3.4
7.5	2	3.5	3.5(w)	8.0	1.8	0	0	4.8	4.3
7.5	2	3.5	1.5(s)	8.0	0	0	0	6.8	7.1
8.5	2	3.5	3.5(w)	8.0	0	0	0	2.7	1.8
8.5	2	3.5	1.5(s)	8.0	0	0	0	2.8	3.4

[a]The letter in parentheses following the modulus of elasticity indicates the design temperature for the asphalt-stabilized layer; i.e., s is average summer temperature of 85 F, and w is average winter temperature of 65 F.

bases were also presented, including definite procedures for the selection of a critical base design thickness. Characterization techniques were also presented to provide necessary estimates of limiting design criteria for the materials proposed for the various pavement layers. The application of the total design approach to the structural design of various types of stabilized base layers is illustrated in an example problem.

The design system presented here is based on a practical interpretation of layered theory that emphasizes the contribution of each individual layer to the behavior of the total pavement structure. The new design system, because of its dependence on layered theory, requires verification through trial use and field observation. This design system, however, offers the basis for correcting and updating by comparing designs based on the theoretical equations against observed pavement performance.

ACKNOWLEDGMENTS

Support for this study was provided by the Texas Highway Department in cooperation with the U.S. Department of Transportation, Federal Highway Administration. The opinions, findings, and conclusions expressed are those of the authors and not necessarily those of the Texas Highway Department or the Federal Highway Administration.

REFERENCES

1. Hadley, W. O. A Comprehensive Structural Design for Stabilized Pavement Layers. Univ. of Texas at Austin, PhD dissertation, Feb. 1972.
2. Hadley, W. O., Hudson, W. R., and Kennedy, T. W. A Comprehensive Structural Design for Stabilized Pavement Layers. Center for Highway Research, Univ. of Texas at Austin, Res. Rept. 98-13, 1972.
3. Warren, H., and Erickmann, W. L. Numerical Computations of Stresses and Strains in a Multiple-Layer Asphalt Pavement System. Chevron Research Corp., Sept. 1963 (unpublished).
4. Hadley, W. O., Hudson, W. R., and Kennedy, T. W. Evaluation and Prediction of the Tensile Properties of Asphalt-Treated Materials. Center for Highway Research, Univ. of Texas at Austin, Res. Rept. 98-9, May 1971.
5. Hadley, W. O., Hudson, W. R., and Kennedy, T. W. A Method of Estimating Tensile Properties of Materials Tested in Indirect Tension. Center for Highway Research, Univ. of Texas at Austin, Res. Rept. 98-7, July 1970.
6. Anagnos, J. N., and Kennedy, T. W. Practical Method of Conducting the Indirect Tensile Test. Center for Highway Research, Univ. of Texas at Austin, Res. Rept. 98-10, Oct. 1971.
7. Hondros, G. The Evaluation of Poisson's Ratio and the Modulus of Materials of a Low Tensile Resistance by the Brazilian (Indirect Tensile) Test With Particular Reference to Concrete. Australian Jour. of Applied Science, Vol. 10, No. 3, Sept. 1959, pp. 243-268.
8. Mitchell, N. B., Jr. The Indirect Tensile Test for Concrete. Materials Research and Standards, ASTM, Vol. 2, No. 10, Oct. 1961, pp. 780-787.
9. Grieb, W. E., and Werner, G. Comparison of the Splitting Tensile Strength of Concrete With Flexural and Compressive Strengths. Public Roads, Vol. 32, No. 5, Dec. 1962, pp. 97-106.
10. Thaulow, S. Tensile Splitting Test and High Strength Concrete Test Cylinders. Jour. American Concrete Institute, Vol. 28, No. 7, Paper 53-38, Jan. 1957, pp. 699-705.
11. Narrow, I., and Ullberg, E. Correlation Between Tensile Splitting Strength and Flexural Strength of Concrete. Jour. American Concrete Institute, Proc. Vol. 60, 1963, pp. 27-37.
12. Mather, B. Stronger Concrete. Highway Research Record 210, 1967, pp. 1-28.
13. Popovics, S. Relations Between Various Strengths of Concrete. Highway Research Record 210, 1967, pp. 67-94.
14. Pfeifer, D. W. Sand Replacement in Structural Lightweight Concrete-Splitting Tensile Strength. PCA Research and Development Laboratory Bull., July 1967, p. 120.

15. Hanson, J. W. Tensile Strength and Diagonal Tension Resistance of Structural Lightweight Concrete. Jour. American Concrete Institute, Proc. Vol. 58, 1961, p. 1.
16. Pendola, H. J., Kennedy, T. W., and Hudson, W. R. Estimation of Factors Affecting the Tensile Properties of Cement-Treated Materials. Center for Highway Research, Univ. of Texas at Austin, Res. Rept. 98-3, Sept. 1969.
17. Anagnos, J. N., Kennedy, T. W., and Hudson, W. R. Evaluation and Prediction of Tensile Properties of Cement-Treated Materials. Center for Highway Research, Univ. of Texas at Austin, Res. Rept. 98-8, Oct. 1970.
18. Hudson, W. R., and Kennedy, T. W. An Indirect Tensile Test for Stabilized Materials. Center for Highway Research, Univ. of Texas at Austin, Res. Rept. 98-1, June 1967.
19. Breen, J. J., and Stephens, J. E. Split Cylinder Test Applied to Bituminous Mixtures at Low Temperatures. Jour. of Materials, ASTM, Vol. 1, No. 1, March 1966.
20. Messina, R. Split Cylinder Test for Evaluation of the Tensile Strength of Asphalt Concrete Mixtures. Univ. of Texas at Austin, MS thesis, Jan. 1966.
21. Hadley, W. O., Hudson, W. R., and Kennedy, T. W. An Evaluation of Factors Affecting the Tensile Properties of Asphalt-Treated Materials. Center for Highway Research, Univ. of Texas at Austin, Res. Rept. 98-2, March 1969.
22. Hadley, W. O., Hudson, W. R., Kennedy, T. W., and Anderson, V. A Statistical Experiment to Evaluate Tensile Properties of Asphalt-Treated Materials. Proc. AAPT, Vol. 38, 1969.
23. Livneh, M., and Shklarsky, E. The Splitting Test for Determination of Bituminous Concrete Strength. Proc. AAPT, Vol. 31, 1962.
24. Anderson, K. O., and Hahn, W. P. Design and Evaluation of Asphalt Concrete With Respect to Thermal Cracking. Proc. AAPT, Vol. 37, 1968, pp. 1-31.
25. Long, R. E. Relationships Between Control Tests for Asphalt Stabilized Materials. Texas A&M Univ., College Station, PhD dissertation, May 1971.
26. Miller, S. P., Kennedy, T. W., and Hudson, W. R. Evaluation of Factors Affecting the Tensile Properties of Lime-Treated Materials. Center for Highway Research, Univ. of Texas at Austin, Res. Rept. 98-4, March 1970.
27. Tullock, W. S., II, Hudson, W. R., and Kennedy, T. W. Evaluation and Prediction of the Tensile Properties of Lime-Treated Materials. Center for Highway Research, Univ. of Texas at Austin, Res. Rept. 98-5, June 1970.
28. Thompson, M. R. Split-Tensile Strength of Lime-Stabilized Soils. Highway Research Record 92, 1965, pp. 69-79.
29. Narain, J., and Prakesh, C. R. Tensile Test for Compacted Soils. Proc. ASCE, Vol. 96. Nov. 1970, pp. 2185-2190.
30. Fang, H. Y., and Chen, W. F. New Method for Determination of Tensile Strength of Soils. Highway Research Record 345, 1971, pp. 62-68.
31. Hilsdorf, H. K., and Kesler, C. E. Fatigue Strength of Concrete Under Varying Flexural Stresses. Jour. American Concrete Institute, Proc. Vol. 63, Oct. 1966, pp. 1059-1075.
32. Moore, R. K., and Kennedy, T. W. Tensile Behavior of Subbase Materials Under Repetitive Loading. Presented at 3rd Internat. Conf. on the Structural Design of Asphalt Pavements, London, 1972.
33. Moore, R. K. Tensile Behavior of Subbase Materials Under Repetitive Loading. Univ. of Texas at Austin, PhD dissertation, 1971.
34. Dormon, G. M., and Metcalf, C. T. Design Curves for Flexible Pavements Based on Layered System Theory. Highway Research Record 71, 1965, pp. 69-84.
35. Hadley, W. O., Hudson, W. R., and Kennedy, T. W. A Nomographic Design Method for Asphalt Stabilized Pavement Layers. Prepared for the 1973 Annual Meeting of AAPT.

CALCULATION OF THE ELASTIC MODULI OF A TWO-LAYER PAVEMENT SYSTEM FROM MEASURED SURFACE DEFLECTIONS

Frank H. Scrivner, Chester H. Michalak, and William M. Moore,
Texas Transportation Institute, Texas A&M University

This report gives the theoretical background and a description of a new computer program, ELASTIC MODULUS II, which is capable of converting deflections measured by the Dynaflect on the surface of a highway pavement-subgrade (two-layer elastic) system to the elastic moduli of the pavement and subgrade. Included in this paper are the solutions of several typical problems. The computer program may eventually become a part of a comprehensive flexible pavement design system now being implemented by the Texas Highway Department.

•IN the early 1960s, following publication of the AASHO Road Test findings (1, 2), the perennial attempt to find a general solution to the flexible pavement structural design problem received a new impetus. On an unprecedented scale there became available masses of data interrelating axle load, accumulated number of axle applications, structural design, and pavement performance.

Shortly thereafter an interim design guide based on the road test findings was written by an AASHO committee for trial use by the member states, and special studies of pavement performance were initiated by several states, including Texas, to find—in their own environments—how the design guide and/or other road test data could best be used locally.

The Texas study, conducted by the Texas Transportation Institute in cooperation with the Texas Highway Department over a period of several years, led to two general conclusions: (a) the most logical way to reduce the AASHO Road Test flexible pavement performance data to a form useful in Texas was to relate these data to the surface deflection (Benkelman beam) data accumulated at the road test and (b) the resulting deflection-performance relation had to be incorporated into an optimizing system capable of producing an array of lowest cost alternate designs, subject to the funds available, other practical constraints, and pavement performance demands inposed on the system by the engineer using it. The cost for each design (or, more accurately, the design strategy) was to include not only the initial construction cost but also all other costs (including the public of traffic delays forced by periodic overlay construction) that could be predicted.

A computer program satisfying the preceding requirements was created at Texas Transportation Institute and turned over to the Texas Highway Department in 1968 (3, 4, 5). At that time, a new research project, involving not only researchers at Texas Transportation Institute and the Texas Highway Department but also those at the Center for Highway Research at Texas University, was initiated for the purpose of carrying on the work of testing and improving the design system, implementing it, and extending it to include rigid pavements (6, 7, 8).

Sponsored by Committee on Strength and Deformation Characteristics of Pavement Sections.

STRUCTURAL SUBSYSTEM

At the core of the flexible pavement system is the empirically derived deflection-performance relation (or subsystem) previously mentioned. It was decided that the reliability of the overall system might be improved if this subsystem were replaced by one based primarily on linear-elastic theory. The use of such a subsystem demands, among other things, that the in situ moduli of typical pavement materials be determined from rapid, economical, nondestructive tests performed on existing roads in the general area where a new pavement is to be constructed. This paper describes a method and a computer program, ELASTIC MODULUS II, for finding such moduli from Dynaflect data in the case of a simple, two-layer system, that is, a pavement where all of the material above a presumably homogeneous subgrade is predominately one material, such as the pavement shown in Figure 1.

The Loading Device (Dynaflect)

Through two steel wheels the trailer-mounted Dynaflect exerts two vertical loads, separated by 20 in. and varying sinusoidally in phase at 8 Hz (Fig. 1). The total load, exerted by rotating weights, varies from 500 lb upward to 500 lb downward. The upward thrust is overcome by the deadweight of the trailer so that the load wheels are always in contact with the pavement. The load-pavement contact areas are small and are considered to be points, rather than areas, in order to simplify the mathematics.

From the symmetry of Figure 1 it can be seen that one load of 1,000 lb can be substituted for the two loads shown, without affecting the vertical motion at points along the line of sensors. For this reason, in what follows only one point load, P, of 1,000 lb, will be considered to be acting on the surface of the pavement.

Notation

Following is a list of the mathematical symbols used in this paper:

- P = vertical force acting at a point in the horizontal surface of a two-layer elastic half-space;
- h = thickness of upper layer;
- E_1 = Young's modulus of upper layer;
- E_2 = Young's modulus of lower layer;
- w = the vertical displacement of a point in the surface;
- r, z = cylindrical coordinates (the tangential coordinate, θ, does not appear because only one load is used as explained, and the resulting vertical deflections are symmetrical about the z-axis);
- m = a parameter;
- x = mr/h;
- $Jo(x)$ = Bessel function of the first kind and zero order with argument x;
- V = a function of m and N (Eqs. 1 and 2); and
- N = a function of E_1 and E_2 (Eq. 2a).

The load P acts downward at the points r = 0 and z = 0. Positive z is measured downward.

Development of a Deflection Equation

A vertical load, P (Fig. 2), is applied at the point, 0, in the horizontal plane surface of a two-layer elastic system. The point of load application is the origin of cylindrical coordinates, r and z. Positive values of z are measured vertically downward.

The thickness of the upper layer is h, and its elastic modulus is E_1. The thickness of the lower layer is infinite, and its elastic modulus is E_2. Poisson's ratio for both layers is taken as one-half.

It can be shown from Burmister's early work in elastic layered systems (9) that the deflection, w, of a surface point at the horizontal distance, r, from the point, 0, is related to the constants, h, E_1, and E_2 by the equation

$$\frac{4\pi E_1}{3P} wr = \int_{x=0}^{\infty} V \times Jo(x)dx \tag{1}$$

where

$x = mr/h$, (1a)

m = a parameter,

$$V = \frac{1 + 4Nme^{-2m} - N^2e^{-4m}}{1 - 2N(1 + 2m^2)e^{-2m} + N^2e^{-4m}}, \text{ and} \tag{2}$$

$$N = \frac{1 - E_2/E_1}{1 + E_2/E_1} = \frac{E_1 - E_2}{E_1 + E_2} \tag{2a}$$

An Approximation of the Deflection Equation

The integration indicated in Eq. 1 must be performed by numerical means. This task is made easier by taking advantage of the fact that (a) as x varies from zero to infinity in the integration process, m varies over the same range, and r and h are held constant; (b) as m varies from zero to infinity, the function V varies monotonically from E_1/E_2 to 1.0; and (c) for practical ranges of the ratio E_2/E_1, V approaches its limiting value of 1.0 at surprisingly low values of m. For example, it was found (Table 1) that, if m is set equal to 10 and E_2/E_1 is restricted to a range of 0 to 1,000, then $V = 1.0 \pm 0.000001$. Thus, we conclude that, for practical purposes, when m is in the range of 0 to 10, V is given by Eq. 2, and, when m is in a range of 10 to infinity, V = 1. This approximation can be expressed algebraically as follows:

$$\int_{x=0}^{\infty} V \times Jo(x)dx \approx \int_{x=0}^{10r/h} V \times Jo(x)dx + \int_{x=10r/h}^{\infty} Jo(x)dx \tag{3}$$

The second integral on the right side of Eq. 3 is equivalent to the difference of two integrals, as indicated by

$$\int_{x=10r/h}^{\infty} Jo(x)dx = \int_{x=0}^{\infty} Jo(x)dx - \int_{x=0}^{10r/h} Jo(x)dx = 1 - \int_{x=0}^{10r/h} Jo(x)dx \tag{4}$$

By making the obvious substitution from Eq. 4 in Eq. 3 we have

$$\int_{x=0}^{\infty} V \times Jo(x)dx \approx \int_{x=0}^{10r/h} V \times Jo(x)dx + 1 - \int_{x=0}^{10r/h} Jo(x)dx, \text{ or}$$

or

$$\int_{x=0}^{\infty} V \times Jo(x)dx \approx 1 + \int_{x=0}^{10r/h} (V - 1)\, Jo(x)dx$$

Comparing the last approximation with Eq. 1, we arrive at the approximation

$$\frac{4\pi E_1}{3P} wr \approx 1 + \int_{x=0}^{10r/h} (V - 1)\, Jo(x)dx \tag{5}$$

where all symbols are as previously defined.

It is of interest to note from Eq. 2 that V = 1 when $E_2 = E_1$ (that is, when the layered system of Fig. 1 degenerates into a homogeneous elastic half-space) and that for this case Eq. 5 reduces to

Figure 1. Relative position of Dynaflect loads and sensors.

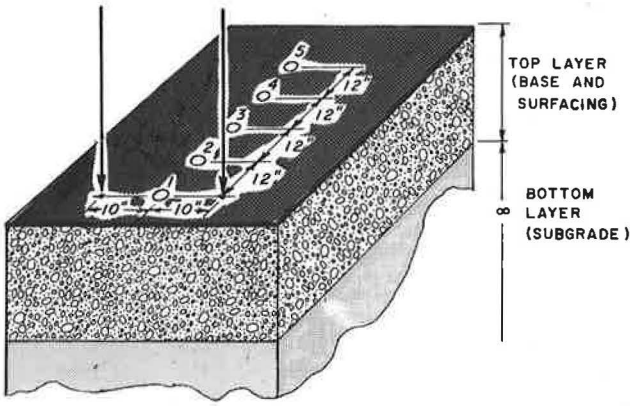

Figure 2. Two-layer elastic system loaded at a point on the surface.

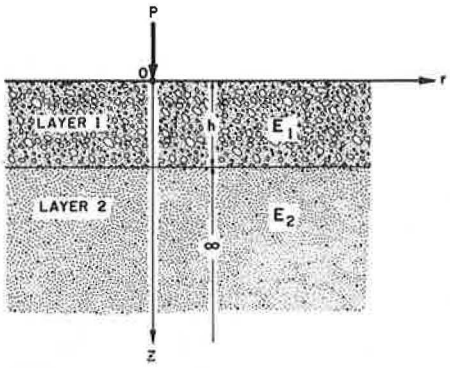

Table 1. Values of the function, V, corresponding to selected values of parameter m and modular ratio E_2/E_1.

	E_2/E_1							
m	0	0.001	0.01	0.1	1	10	100	1,000
0.0	Infinite	1,000	100	10	1	0.1	0.01	0.001
0.1	6,012	855.6	98.14	9.967	1	0.1006	0.01065	0.001655
0.5	50.49	47.94	32.98	8.056	1	0.1542	0.06727	0.05854
1.0	7.382	7.363	6.826	4.112	1	0.3250	0.2491	0.2414
3.0	1.137	1.137	1.134	1.110	1	0.9058	0.8888	0.8869
5.0	1.006	1.006	1.005	1.005	1	0.9955	0.9946	0.9945
10.0	1.000001	1.000001	1.000001	1.000001	1	0.9999993	0.9999991	0.9999991
Infinite	1	1	1	1	1	1	1	1

$$\frac{4\pi E_1}{3P} wr \approx 1$$

The correct equation for this case, according to Timoshenko (10), is

$$\frac{4\pi E_1}{3P} wr = 1$$

Thus, for the homogeneous case Eq. 5 becomes exact.

NUMERICAL INTEGRATION OF DEFLECTION EQUATION

To use Eq. 5, we had to employ some form of numerical integration process for evaluating the integral in that equation. The method known as Simpson's rule was selected (11). This procedure required that a small but finite increment, Δx, be chosen and that the integrand be calculated at $x = 0$, $x = \Delta x$, and $x = 2\Delta x$ over the specified range of integration. The smaller the value assigned to Δx, the greater would be the accuracy of the result; on the other hand, the larger the value of Δx, the less would be the required computer time. Thus a compromise between computer time and accuracy had to be made.

Because the integral of Eq. 5 is the product of the factor V - 1, which is a function of m and N, and Jo(x)—which is a function of $x = mr/h$ (Eq. 1a)—two safeguards against inaccurate results had to be incorporated into the program:

1. Δm had to be small enough to ensure a sufficiently accurate numerical representation of the function V, and
2. Δx had to be small enough to ensure an accurate numerical representation of the function Jo(x).

After some study of the numerical values of V given in Table 1 and of the values of Jo(x) available from numerous sources (12), the following rules were incorporated into the computer program for solving Eq. 5:

1. In the range $m = 0$ to $m = 3$, $\Delta m \leq 0.01$ (in FORTRAN, DELM1 .LE. XK1.).
2. In the range $m = 3$ to $m = 10$, $\Delta m \leq 0.10$ (in FORTRAN, DELM2 .LE. XK2.).
3. In the entire range of x from 0 r/h to 10 r/h, not less than 61 values of Jo(x) are computed as x increases from any value $x = c$ to the value $x = c + 3$. This also ensures that the number of values of Jo(x) computed between successive zeroes of that alternating function exceeds 61 (in FORTRAN, XNO = 61).

Because Δx and Δm are interdependent according to Eq. 1a, that is,

$$\Delta x = \Delta m \, r/h \tag{1b}$$

the computer program had to ensure that the rules previously given were consistent with Eq. 1b. The accuracy of the solutions obtained (or the computer time used) can be changed by altering the values assigned to the FORTRAN variables XK1, XK2, and XNO.

As an example of how Eq. 5 is used in ELASTIC MODULUS II to find pavement and subgrade moduli, consider the following conditions.

Let us assume that w_1 has been measured on the surface of a pavement structure at the distance r_1 from either Dynaflect load and w_3 at the distance r_3. The thickness, h, of the pavement is known.

Now let F represent the function on the right side of Eq. 5. We may then write two equations:

$$\frac{4\pi E_1}{3P} w_1 r_1 \approx F(E_2/E_1, \, r_1/h) \tag{6a}$$

$$\frac{4\pi E_1}{3P} w_3 r_3 \approx F(E_2/E_1, \, r_3/h) \tag{6b}$$

By dividing Eq. 6a by Eq. 6b, we obtain

$$\frac{w_1 r_1}{w_3 r_3} = \frac{F(E_2/E_1,\ r_1/h)}{F(E_2/E_1,\ r_3/h)} \tag{7}$$

where E_2/E_1 is the only unknown.

By a convergent process of trial and error, a value of E_2/E_1 usually can be found that satisfies Eq. 7 to the desired degree of accuracy. After this has been done, E_1 is calculated from Eq. 6a, and finally E_2 is found from the relation

$$E_2 = E_1\left(\frac{E_2}{E_1}\right)$$

Accuracy Check

As was mentioned previously, a point load was substituted in ELASTIC MODULUS II for the area loads exerted by the Dynaflect. To check the effect of this assumption on accuracy, as well as the effect of the approximations described previously, we used the following procedure.

The contact area of each load wheel was measured approximately by inserting light-sensitive paper between each wheel and the pavement, running the Dynaflect for a short time in strong sunlight, and removing the paper and measuring the unexposed areas.

From these measurements it was concluded that each 500-lb load could be represented by a uniform pressure of 80 psi acting on a circular area with a radius of 1.41 in. Furthermore, because of the symmetry of the load-geophone configuration, it was reasoned that the effect of both loads could be represented by a pressure of 160 psi acting on one circular area of the radius given previously (1.41 in.).

The surface deflections w_1 and w_3 (Fig. 1), occurring at the distances r = 10 in. and $r = \sqrt{10^2 + 24^2} = 26$ in. from the center of the circle, could then be calculated from the program BISTRO, written by Koninklijke/Shell-Laboratorium, Amsterdam, and compared with deflections obtained by the program ELASTIC MODULUS II modified slightly to receive as inputs E_1, E_2, h, and r and to print out w_1 and w_3.

The two programs were compared as described previously over a range of the ratio E_1/E_2 from 0.1 to 1,000 and a range of the thickness h from 5 to 40 in. The results are given in Table 2 in the same manner that Dynaflect deflections are recorded, that is, in mils to two decimal places.

The table shows near-perfect agreement in the range $1 \leq E_1/E_2 \leq 1{,}000$, for which the pavement is stiffer than the subgrade. On the other hand, with the subgrade much stiffer than the pavement ($E_1/E_2 = 0.1$, Table 2), the agreement was not as good. In addition, upheavals occurred, as indicated by the negative signs of some of the deflections. In these cases, the deflected surface is very irregular, and Dynaflect data from such a pavement would be difficult to interpret because this device is not equipped to distinguish phase differences between load and geophone.

Because most pavements of the type shown in Figure 1 are obviously intended to be stiffer than their subgrades, and, in view of the fact that irregular basin shapes are seldom encountered in practice, it is concluded from the data given in Table 2 that ELASTIC MODULUS II represents the theory of elasticity with sufficient accuracy to accomplish the purpose for which it was designed.

NON-UNIQUE SOLUTIONS

To investigate the possibility that the use of the program could lead to more than one solution (that is, to more than one value of the ratio E_1/E_2) or, perhaps, to no solution at all in some cases, ELASTIC MODULUS II was modified slightly to receive as inputs selected values of E_1/E_2 and the layer thickness h and to compute the corresponding ratio $w_1 r_1/w_3 r_3$ (Eq. 7). The results of these computations were plotted as contours of the layer thickness (Fig. 3). The range of input data was limited to the largest range that might be expected from field deflection tests made on real highways of the type shown in Figure 1.

Figure 3. Contours of pavement thickness plotted as a function of the ratios E_1/E_2 and w_1r_1/w_3r_3.

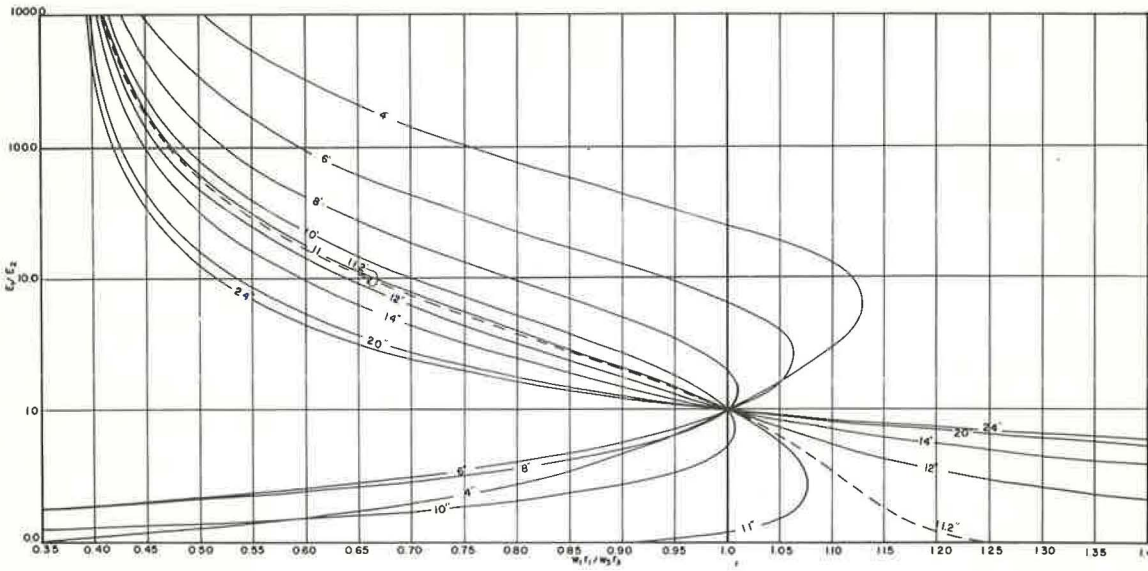

Table 2. Comparison of ELASTIC MODULUS II and BISTRO.

Young's Modulus of Upper Layer (psi)	Young's Modulus of Lower Layer (psi)	E_1/E_2	Thickness (in.)	Computed Deflections (mil) w_1 ELASTIC MODULUS II	w_1 BISTRO	w_3 ELASTIC MODULUS II	w_3 BISTRO
10,000,000	10,000	1,000	5	0.99	0.99	0.81	0.81
			10	0.52	0.52	0.48	0.48
			20	0.26	0.26	0.26	0.26
			40	0.13	0.13	0.13	0.13
1,000,000	10,000	100	5	1.86	1.85	1.09	1.09
			10	1.07	1.07	0.84	0.84
			20	0.57	0.57	0.51	0.51
			40	0.30	0.30	0.28	0.28
100,000	10,000	10	5	2.65	2.65	0.98	0.98
			10	1.94	1.93	1.06	1.06
			20	1.20	1.20	0.86	0.86
			40	0.74	0.74	0.56	0.56
10,000	10,000	1	5	2.39	2.39	0.92	0.92
			10	2.39	2.39	0.92	0.92
			20	2.39	2.39	0.92	0.92
			40	2.39	2.39	0.92	0.92
1,000	10,000	0.1	5	-0.01	-0.04	0.80	0.80
			10	-0.15	-0.06	0.35	0.35
			20	7.45	7.52	0.42	0.42
			40	14.90	14.90	1.60	1.60

Note: For ELASTIC MODULUS II, there is a point load of 1,000 lb. For BISTRO, circular loaded area has a radius of 1.41 in., a pressure of 160 psi, and a load of 1,000 lb. For both programs, vertical deflection was computed at the points r = 10 in. (z = 0) and r = 26 in. (z = 0).

To facilitate interpretation, Figure 3 has been divided into four quadrants. For example, by referring to quadrants I and II (Fig. 3) it can be seen that, if the measured inputs to ELASTIC MODULUS II satisfy the inequalities, $w_1r_1/w_3r_3 > 1$ and $h \geq 11.2$ in., a unique solution satisfying the inequality $E_1/E_2 < 1$ exists, and in this case the program finds and prints the two moduli. If, on the other hand, $w_1r_1/w_3r_3 > 1$ (as before) but $h < 11.2$ in., the possibility of two solutions exists; also there may be no solution if the measured ratio w_1r_1/w_3r_3 is sufficiently great. In this case, i.e., $w_1r_1/w_3r_3 > 1$ and $h < 11.2$ in., the program abandons the search for a solution and prints the message NO UNIQUE SOLUTION.

By examining quadrants III and IV, it can be concluded that, if $w_1r_1/w_3r_3 < 1$ and $h \geq 11.2$ in., a unique solution satisfying the inequality $E_1/E_2 > 1$ exists. In this case the program finds the solution and prints the two moduli. On the other hand, if $w_1r_1/w_3r_3 < 1$ as before but $h < 11.2$ in., there are two possible solutions: one in quadrant III for $E_1/E_2 > 1$ and another in quadrant IV for $E_1/E_2 < 1$. Of these two solutions, the one in quadrant III, representing a pavement whose elastic modulus is greater than that of the subgrade, is the more probable; therefore, the program seeks out the quadrant III solution, prints the corresponding moduli, and ignores the quadrant IV solution.

The information deduced from Figure 3 and used in the control of the program ELASTIC MODULUS II is summarized in Table 3.

EXAMPLES OF SOLUTIONS OBTAINED BY ELASTIC MODULUS II

In May 1968, Dynaflect deflections were measured at 10 points in the outer wheelpath on each of several 500-ft sections of highways in the vicinity of College Station, Texas. Some of these data, including thicknesses obtained by coring at five points in each section, were used as inputs to the computer program discussed here for the purpose of illustrating its use in obtaining the elastic moduli of pavements and subgrades. The results are summarized in Tables 4 and 5, and an example of the computer printout, in the standard format of the program, is shown in Figure 4. In the computer printout, the readings of each of the five geophones at each test station are given, although only the deflections w_1 and w_3 were actually used in estimating the moduli E_1 and E_2.

Tables 4 and 5 are arranged in descending order of the magnitude of the average modulus of pavement and subgrade respectively. In comparing these two tables it is of interest to note that the within-section variability of the pavement modulus, as indicated by the standard deviation, is generally greater, both in absolute value and in relation to the section average, than that of the subgrade. In addition, it is apparent that the range of E_1 (14,000 to 314,100 psi) is much greater than the range of E_2 (11,100 to 19,100 psi). It is also noteworthy that the pavement of section 12 (Table 4) had an average modulus (14,900 psi) of approximately the same magnitude as that of its subgrade (14,000 psi).

The low pavement modulus found for section 12 may be due to the relatively poor quality of the major component of the pavement, a sandstone that, according to local engineers, has in some cases performed poorly. In any event the surfacing of this section had been overlaid (because of map cracking) shortly before it was tested in 1968; it again developed severe map cracking that required sealing in 1970. The seal coat failed to arrest the progress of surface deterioration, and the section was again overlaid with 1 in. of hot-mix asphaltic concrete in 1971. In short, the contrast between the stiffness of the surfacing material and that of the base seems to be at the root of the trouble in this section.

The greater within-section uniformity of the calculated foundation modulus may be due in part to the necessary assumption of infinite foundation depth. This assumption would seem to lead to the association of relatively large changes in surface deflections with relatively small changes in foundation modulus.

The last column in Tables 4 and 5 can be explained by referring to Figure 4, which shows that replicate measurements, designated A and B, were taken at each of the numbered stations. The stations were selected at intervals of 100 ft, and the replicate measurements at each station were taken at points separated by only 10 ft. The rep-

Table 3. ELASTIC MODULUS II information summary.

Measured Input Data				
w_1r_1/w_3r_3	Thickness (in.)	Unique Solution	Layer Having the Greater Modulus	Program Printout
>1	>11.2	Yes	Subgrade	Subgrade and pavement moduli
>1	<11.2	No	May be either	NO UNIQUE SOLUTION[a]
<1	>11.2	Yes	Pavement	Subgrade and pavement moduli
<1	<11.2	No	May be either, but the more probable of two possible solutions is selected	Subgrade and pavement moduli for solution having $E_1/E_2 > 1$

[a]When the experimental data $w_1r_1/w_3r_3 > 1$ and h is < 11.2 in., some cases can arise for which no solution at all is possible.

Table 4. Average pavement modulus for flexible pavement sections.

Test Section	Pavement Materials and Thicknesses		Pavement Thickness		Pavement Modulus			
	Surfacing	Base	Average Value (in.)	Standard Deviation	Number of Solutions[a]	Average Value (psi)	Standard Deviation (psi)	Replication Error (psi)
15	1.2-in. asphalt concrete	14.0-in. cement-stabilized limestone	15.2	1.2	10	314,100	75,200	9,800
4	0.5-in. seal coat	7.5-in. asphalt-stabilized gravel	8.0	0.4	4	110,500	90,400	3,300
16	1.0-in. asphalt concrete	6.5-in. asphalt emulsion stabilized gravel	7.5	0.4	10	109,300	19,700	3,600
17	0.5-in. seal coat	7.8-in. iron ore gravel	8.3	0.7	10	81,900	47,700	7,400
5	0.5-in. seal coat	11.5-in. lime-stabilized sandstone	12.0	2.8	10	23,800	15,400	4,200
3	0.5-in. seal coat	12.0-in. red sandy gravel	12.5	1.0	10	23,700	11,600	2,300
12	3.7-in. asphalt concrete	16.2-in. sandstone	19.9	0.5	10	14,900	3,300	1,200

Note: Deflection measurements were made May 21, 1968, near College Station, Texas.

[a]Measurements were made at 10 locations in each section. Fewer than 10 solutions occur in cases where $w_1r_1/w_3r_3 > 1$ and h < 11.2 in., as given in Table 3.

Table 5. Average subgrade modulus for flexible pavement sections.

Test Section	Thickness Investigated (in.)	Subgrade Material		Subgrade Modulus			
		Description	Formation	Number of Solutions[a]	Average Value (psi)	Standard Deviation (psi)	Replication Error (psi)
15	32	Red sandy clay, some gravel	Stone City	10	19,100	790	390
3	23	Sand over clay	Spiller sandstone, member of Cook Mountain formation	10	19,000	1,300	370
5	24	Tan sandy clay	Caddell	10	14,800	1,600	540
12	22	Black stiff clay	Lagarto	10	14,000	980	250
4	25	Gray sandy clay	Spiller sandstone, member of Cook Mountain formation	4	11,800	1,270	320
17	21	Gray sandy clay	Spiller sandstone, member of Cook Mountain formation	10	11,400	1,200	210
16	18	Brown clay	Alluvium deposit of Brazos River	10	11,100	530	120

Note: Deflection measurements were made May 21, 1968, near College Station, Texas.

[a]Measurements were made at 10 locations in each section. Fewer than 10 solutions occur in cases where $w_1r_2/w_3r_3 > 1$ and h < 11.2 in., as given in Table 3.

lication error at any station is defined as one-half the difference between the two measurements, whereas the replication error for the entire section is obtained by squaring and adding the station replication errors, dividing by the number of stations involved, and taking the square root of the result.

By noting the differences between the replication errors and the standard deviations given in Tables 4 and 5, we can compare the variability encountered in a distance of 10 ft with the variability found over a distance 50 times greater. With one exception, the standard deviation of a section was larger than its replication error by a factor ranging from 2 to 8. In the one exception (section 4 in Table 4), only four solutions could be found, and these were at two stations differing greatly in the calculated base modulus: In this instance, the standard deviation was 27 times greater than the replication error.

ADJUSTMENT OF MODULI FOR PRACTICAL USE IN PAVEMENT DESIGN

As previously noted, the elastic moduli estimated by the computer program are based on deflections produced and measured by the Dynaflect system. Correlation studies of Dynaflect deflections with those produced by a 9,000-lb dual-tired wheel load and measured by means of the Benkelman beam on highways in Illinois and Minnesota in 1967 (13) indicated that the 9,000-lb wheel load deflection could, with reasonable accuracy, be estimated from the Dynaflect deflection, w_1, by multiplying w_1 by 20.

But the peak-to-peak load of the Dynaflect is 1,000 lb; thus, one would expect that the multiplying factor would be about 9 rather than 20, as was found by actual field experience.

Various explanations could be advanced to explain this discrepancy. However, they would not alter the fact, brought out by the correlation study, that, if one desires to use the values of E_1 and E_2 found from Dynaflect deflections to calculate the static, rebound deflection of a linear-elastic-layered system acted on by a 9,000-lb wheel load, then he should approximately halve these moduli before using them in his calculations.

CONCLUSIONS

The following conclusions are supported by the study results:

1. The accuracy of ELASTIC MODULUS II was tested against the widely used program BISTRO with favorable results (Table 2).
2. Within-section variability of the upper (base and surfacing) layer was greater, both in absolute value and in relation to the section average, than that of the subgrade (Tables 4 and 5).
3. With one exception, where the volume of data was insufficient to permit valid comparisons, the variability of a base (or subgrade) modulus encountered in a distance of 10 ft within a section ranged from $\frac{1}{8}$ to $\frac{1}{2}$ of the variability found over the full 500-ft length of the section. In the one exception (out of 14 comparisons) the ratio was 1 to 27 (compare last two columns of Tables 4 and 5).

ACKNOWLEDGMENT

The research reported here was done in a project sponsored by the Texas Highway Department and the Federal Highway Administration. The opinions, findings, and conclusions expressed are those of the authors and not necessarily those of the Department of Transportation, Federal Highway Administration.

REFERENCES

1. The AASHO Road Test: Report 5—Pavement Research. HRB Spec. Rept. 61E, 1962, 352 pp.
2. The AASHO Road Test, Proceedings of a Conference Held May 16-18, 1962, St. Louis, Mo. HRB Spec. Rept. 73, 1962, 438 pp.
3. Scrivner, F. H., Moore, W. M., McFarland, W. F., and Carey, G. R. A Systems Approach to the Flexible Pavement Design Problem. Texas Transportation Institute, Texas A&M Univ., College Station, Res. Rept. 32-11, 1968.

4. Scrivner, F. H., and Moore, W. M. An Empirical Equation for Predicting Pavement Deflections. Texas Transportation Institute, Texas A&M Univ., College Station, Res. Rept. 32-12, 1968.
5. Scrivner, F. H., and Michalak, C. H. Flexible Pavement Performance Related to Deflections, Axle Applications, Temperatures and Foundation Movements. Texas Transportation Institute, Texas A&M Univ., College Station, Res. Rept. 32-13, 1969.
6. Hudson, W. R., McCullough, B. F., Scrivner, F. H., and Carey, G. R. Systems Analysis Method for Pavement Structures. Jour. of the Struct. Div., Proc. ASCE, Vol. 97, No. ST1, Jan. 1971, pp. 81-97.
7. Texas Highway Department Pavement Design System, Part I Flexible Pavement Designer's Manual. Highway Design Division, Texas Highway Department, Austin, 1972.
8. Kher, R. K., Hudson, W. R., and McCullough, B. F. Comprehensive Systems Analysis for Pavements. Highway Research Record 362, 1971, pp. 1-8.
9. Burmister, D. M. The Theory of Stresses and Displacements in Layered Systems and Applications to the Design of Airport Runways. HRB Proc., 1943, p. 130.
10. Timoshenko, S., and Goodier, J. N. Theory of Elasticity. McGraw-Hill Book Company, Inc., New York, 1951, p. 365.
11. Eshback, O. W. Handbook of Engineering Fundamentals, 2nd Ed. John Wiley and Sons, New York, 1953, pp. 2-114.
12. CRC Handbook of Tables for Mathematics, 3rd Ed. The Chemical Rubber Company, Cleveland.
13. Scrivner, F. H., Poehl, R., Moore, W. M., and Phillips, M. B. Detecting Seasonal Changes in Load-Carrying Capabilities of Flexible Pavements. NCHRP Rept. 76, 1969, 37 pp.

DISCUSSION

H. Y. Fang and T. J. Hirst, Lehigh University

The authors have presented an interesting method for computing the elastic moduli of a two-layer pavement-subgrade system based on Dynaflect surface deflections. The writers wish to provide additional information concerning a similar investigation undertaken by Lehigh University.

A simple relation, developed by Fang and Schaub (14) and based on the work of Boussinesq and Burmister, showed that the modulus of subgrade section K_ε, and Young's modulus of elasticity of the subgrade E_s, can be computed from Benkelman beam surface deflections if the thickness of the pavement is known. The relations among surface deflection, Young's modulus of elasticity, and modulus of subgrade reaction (based on a 30-in. diameter rigid plate) are as follows:

$$E_s = 0.477 \frac{P\beta}{\delta} \tag{8}$$

$$K_\varepsilon = 0.027 \frac{P\beta}{\delta} \tag{9}$$

where

β = coefficient of deflection that is a function of pavement thickness,
δ = pavement surface deflection determined by Benkelman beam, and
K_ε, E_s, P = as previously defined.

Good agreement between theoretical and experimental data from the AASHO Road Test Loop 1 was observed.

Further studies of the relation between both Benkelman beam and Dynaflect surface deflections and the elastic properties of the pavement and subgrade have been con-

Figure 4. Computer printout for section 16.

TEXAS HIGHWAY DEPARTMENT

DISTRICT 17 - DESIGN SECTION

DYNAFLECT DEFLECTIONS AND CALCULATED ELASTIC MODULI

THIS PROGRAM WAS RUN - 07/15/71

DIST.	COUNTY
17	BRAZOS

CONT.	SECT.	JOB	HIGHWAY	DATE	DYNAFLECT
1560	1	1	FM 1687	5-21-68	1

PAV. THICK. = 7.50 INCHES

ASPHALT SURFACING 1.00 ASPH EMUL STAB GRAVL 6.50

BROWN CLAY SUBGRADE 0.0

STATION	W1	W2	W3	W4	W5	SCI	** ES **	** EP **	REMARKS
1 - A	2.160	1.500	0.960	0.660	0.520	0.660	10900.	86100.	
1 - B	2.130	1.530	0.960	0.650	0.510	0.600	10900.	93000.	
2 - A	1.920	1.410	0.930	0.640	0.490	0.510	11500.	140500.	
2 - B	1.860	1.350	0.900	0.630	0.500	0.510	11800.	144300.	
3 - A	2.040	1.470	0.930	0.630	0.490	0.570	11300.	102300.	
3 - B	2.070	1.500	0.960	0.650	0.500	0.570	11000.	109200.	
4 - A	2.220	1.620	1.020	0.670	0.490	0.600	10300.	97000.	
4 - B	2.220	1.590	1.020	0.650	0.490	0.630	10300.	97000.	
5 - A	1.980	1.380	0.900	0.610	0.470	0.600	11700.	103800.	
5 - B	1.980	1.440	0.930	0.610	0.460	0.540	11400.	120100.	
AVERAGES	2.058	1.479	0.951	0.640	0.492	0.579	11110.	109330.	
STANDARD DEVIATION						0.049	528.	19723.	
NUMBER OF POINTS IN AVERAGE =						10	10	10	

W1 DEFLECTION AT GEOPHONE 1
W2 DEFLECTION AT GEOPHONE 2
W3 DEFLECTION AT GEOPHONE 3
W4 DEFLECTION AT GEOPHONE 4
W5 DEFLECTION AT GEOPHONE 5
SCI SURFACE CURVATURE INDEX (W1 MINUS W2)
ES ELASTIC MODULUS OF THE SUBGRADE FROM W1 AND W3
EP ELASTIC MODULUS OF THE PAVEMENT FROM W1 AND W3

Figure 5. Benkelman beam and Dynaflect values.

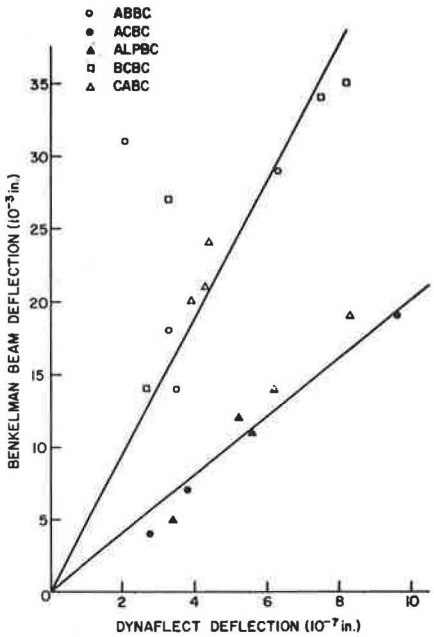

Figure 6. Predicted versus measured subgrade modulus.

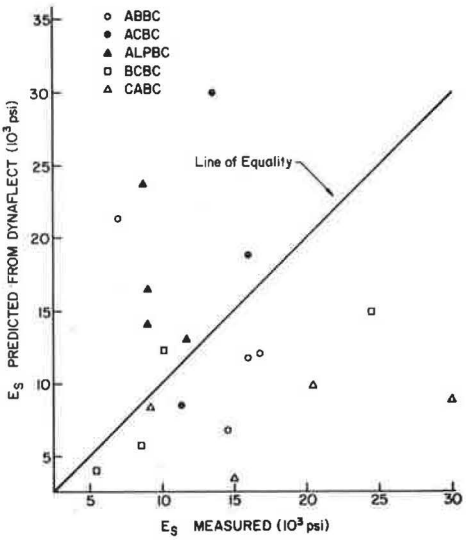

ducted on various pavement sections in southeastern Pennsylvania (15). Of particular interest has been the observation that the relation between Benkelman beam and Dynaflect deflections is base-type dependent. Figure 5 shows a comparison of Benkelman beam and Dynaflect deflections for 19 different in-service flexible pavements. The variables in this investigation were base type [aggregate bituminous (ABBC), aggregate cement (ACBC), aggregate-lime-pozzolan (ALPBC), bituminous concrete (BCBC), crushed aggregate (CABC)] and subgrade support. As may be seen from Figure 5, although some scatter is evident, the data occur in two distinct groups. One group contains crushed aggregate and asphalt-stabilized bases, whereas the other group consists of lime and cement-stabilized base materials. Least-squares orthogonal regressions on the data yielded the following linear equations:

For lime- and cement-stabilized bases

$$\Delta_1 = 4.85 \times 10^4 \, \Delta_2 \tag{10}$$

For crushed aggregate and asphalt-stabilized bases

$$\Delta_1 = 2.02 \times 10^4 \, \Delta_2 \tag{11}$$

where

Δ_1 = Benkelman beam deflection (in.), and
Δ_2 = Dynaflect deflection (in.).

By utilizing the correlations shown in Figure 5 and Eqs. 10 and 11 in conjunction with Eqs. 8 and 9, a Young's modulus of elasticity of the subgrade may be computed from the Dynaflect deflections. Figure 6 shows a comparison between the computed modulus and that measured on the subgrade (30-in. diameter plate load test). Again, scatter in the data is noticeable, which may be attributed to many causes including the assumptions of the analysis and the inherent difficulties associated with large-diameter field-plate loading tests. However, in spite of the scatter, the influence of base type on the computed results is evident. Generally, subgrade moduli predicted for pavements with lime- or cement-treated bases are higher than those for asphalt and crushed aggregate bases. Similar results were obtained for the modulus of subgrade reaction.

Determination of subgrade properties by conventional plate loading tests is a most time-consuming and expensive procedure. Alternate means of establishing the strength and deformation properties, such as those utilizing Benkelman beam and Dynaflect deflections, are badly needed. Their use is to be encouraged; however, care must be taken to ensure that the influence of the various pavement components is properly recognized.

References

14. Fang, H. Y., and Schaub, J. H. Analysis of the Elastic Behavior of Flexible Pavements. Proc. 2nd Internat. Conf. on the Struct. Design of Asphalt Pavements, 1967, pp. 719-729.
15. Hirst, T. J., Fang, H. Y., and Schmidt, D. W. Soil Support and Structural Coefficients for Flexible Pavements in Pennsylvania. Fritz Engineering Laboratory, Lehigh Univ., Rept. 350.5, Oct. 1972.

CHARACTERIZATION OF SUBGRADE SOILS IN COLD REGIONS FOR PAVEMENT DESIGN PURPOSES

Arthur T. Bergan, University of Saskatchewan; and
C. L. Monismith, Institute of Transportation and Traffic Engineering, University of California, Berkeley

This paper discusses the assessment of the effects of freezing and thawing on the stiffness of subgrade soils in an environment representative of the north central portion of the North American continent. Subgrade samples were taken in the fall of 1970 and in the spring of 1972 from a road in the province of Saskatchewan. These samples were used to determine in situ suction and resilient moduli values representative of those existing in the spring and the fall, and a laboratory test was developed to duplicate these conditions. Moduli of the undisturbed samples obtained during the spring were considerably lower then those for samples obtained in the fall, whereas moduli of the remolded samples were considerably higher than those of the undisturbed samples, probably reflecting the presence of secondary structure in the undisturbed samples. After two freeze-thaw cycles on the remolded samples, moduli were obtained similar to the values obtained for the 1972 spring samples. Suction values obtained for the undisturbed samples were lower than for remolded samples. In situ suction values appear to range between 5 and 30 psi, indicating the need for precise techniques for measurement. Applicability of the psychrometer for determination of in situ suction values was investigated; this device does not appear sufficiently accurate to measure suctions in this low range.

•PREDICTION of the response of asphalt pavements to moving wheel loads, which in turn permits an estimate to be made of fatigue damage caused by repetitive stressing in the asphalt-bound layer, requires, among a number of factors, an estimate of the dynamic or resilient response characteristics of the untreated materials comprising the pavement section. One such procedure presented by Kasianchuk (5) makes use of a resilient modulus for subgrade soils determined by means of a repeated load triaxial compression test (13). In a recent investigation (2) this procedure was used to consider fatigue distress and applied to the analysis of an existing pavement in the province of Saskatchewan. The original method was developed for conditions in which no freezing of the subgrade occurs; therefore, application of this method to a northern environment such as Saskatchewan requires consideration of the effects of freezing and thawing on the response of soils. This paper outlines the problems and describes a method for characterizing the subgrade soil for a specific section of highway, Regina to Lumsden, in Saskatchewan for such conditions.

OUTLINE OF STUDY

In a northern environment such as experienced in central Canada, the deflection response of an asphalt pavement consisting of comparatively thin asphalt concrete layer (approximately 4 in.) overlaying untreated aggregate base and subbase varies

Sponsored by Committee on Strength and Deformation Characteristics of Pavement Sections.

considerably throughout the year and will be influenced markedly by the stiffness characteristics of the subgrade soil. Figure 1 shows the seasonal variation in Benkelman beam deflection of a section of highway between Regina and Lumsden in Saskatchewan. Based on earlier studies (14), it can be argued that, if the deflection response could be predicted from laboratory tests, the fatigue distress that had actually developed in this highway (Fig. 2) could be estimated.

Accordingly, the purposes of the study reported in this paper were to determine the in situ resilient moduli of the subgrade in the spring and in the fall and to develop a laboratory procedure that would duplicate both conditions. This was accomplished by studying the subgrade soil from the Regina-to-Lumsden highway, which had been in service for several years. This road was selected for investigation because its subgrade is relatively uniform, and, as noted earlier, the study formed a part of a larger fatigue simulation program (2) to attempt to predict the distress shown in Figure 2.

During the fall of 1970 and again during the spring of 1972, 12 sites were selected for detailed study. At these sites block samples of asphalt concrete, disturbed samples of base and subbase, and undisturbed samples of the lacustrine clay subgrade were obtained. This paper is concerned with the test program for the subgrade soils, a summary of which is as follows: Two or three $4\frac{1}{2}$-in. diameter Shelby tube samples were taken at each site. Sample 1 was located 0 to 2 ft below top of subgrade, sample 2 was 2 to 4 ft below top of subgrade, and sample 3 was 4 to 6 ft below top of subgrade. All samples were taken in outer wheelpath, right-hand lane. The testing consisted of plastic and liquid limits tests, moisture content and density tests, and suction and resilient modulus tests.

Water content and dry density test results for all samples are shown in Figure 3. In this figure it is interesting to note that 45 samples exhibited water contents greater than the optimum water content based on the standard AASHO compaction test, whereas only four had less than optimum water content. The average plastic and liquid limits for this soil are 30 and 75 percent respectively. When the subgrade was constructed in 1961, the soil was placed several percent dry of the standard AASHO optimum water content and at a dry density ranging from 80 to 90 lb/ft^3. The test results indicate that a significant increase in water content in the subgrade has taken place since construction. Test results, however, do not indicate a difference in water content and dry density between the fall of 1970 and the spring of 1972.

RESILIENT MODULUS TESTING

Repeated load triaxial tests were performed on all samples to determine resilient moduli. Specimens 2.8 in. in diameter by about 6.0 in. in length were used for the first few tests; however, it was soon concluded that more uniform results could be obtained by using specimens 4 in. in diameter and 8 in. long. During the repeated load testing lateral and axial deflections were measured using a Linear Variable Displacement Transducer (LVDT). In a recent study, Dehlen (3) found that 1,000 stress repetitions were sufficient to condition the specimen to avoid changes in axial deflection because of end imperfections. The same procedure was tried and found adequate for the Regina clay samples. After a stress level change it was observed that 50 or 100 stress repetitions were sufficient to eliminate significant changes in modulus on further applications of repeated loads, which is similar to the results observed for glacial till material by McLeod (7).

Load was applied for 0.1 sec at 20 cycles per minute, and samples were tested at a confining pressure of 2 psi and a range in deviator stress of 1 to 5 psi. These stresses were selected based on analysis of typical stress conditions in the subgrade as determined by analytical techniques (2).

Results of the resilient moduli tests at $\sigma_3 = 2$ psi and $\sigma_d = 5$ psi are shown in Figure 4. Although there is considerable scatter in the data, most of the moduli are in the range 3,000 to 10,000 psi, with an average value of 8,200 psi for the fall of 1970 and an average value of 6,300 psi for the spring of 1972. These results agree reasonably well with observed pavement response in cold regions where a peak deflection is experienced in the spring probably because of a decrease in subgrade modulus (Fig. 1).

Figure 1. Benkelman beam deflection.

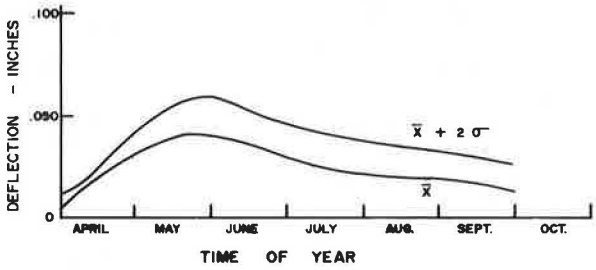

Figure 2. Fatigue and transverse cracking.

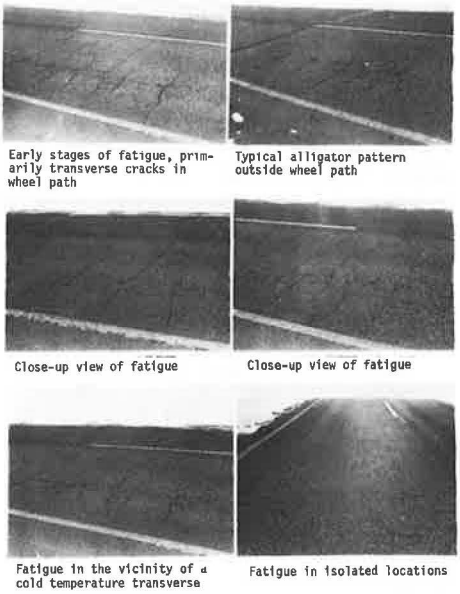

Figure 3. Moisture-density conditions of test road samples.

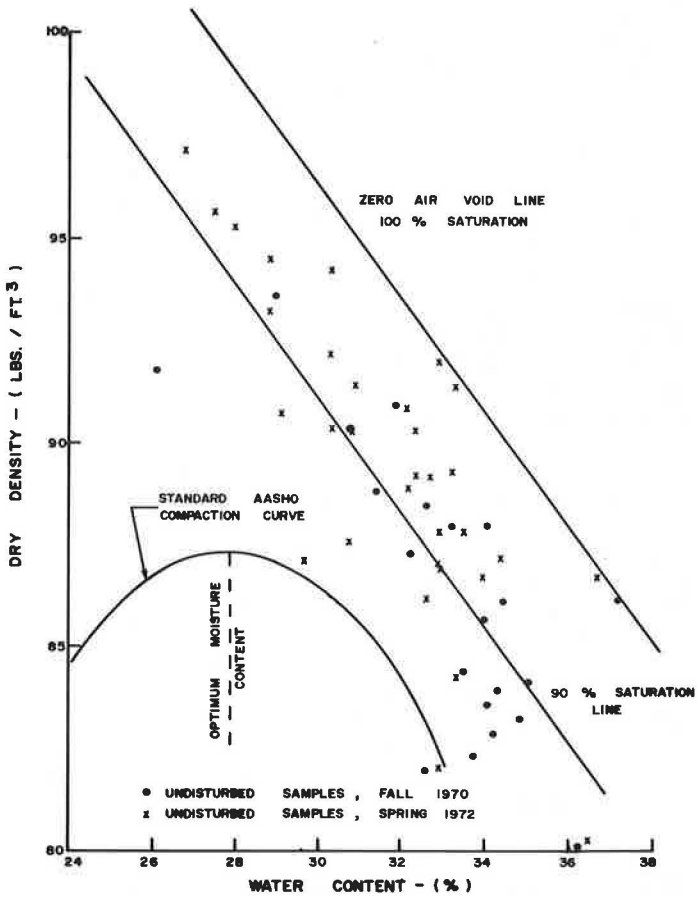

After the samples had been tested, some were then frozen and retested. Prior to freezing, the samples were wrapped in a plastic film, placed in a Zonolite-insulated container, and surcharged with a 5-lb weight. The samples were frozen for 8 hours at 0 F and then thawed for 8 hours and retested. Confining pressure was not applied during freezing, nor were repeated loads applied during freezing. Typical results, which are shown in Figure 5, indicate the resilient modulus dropped considerably after one freeze-thaw cycle. The results after freeze-thaw (Fig. 5) were taken after 1,000 stress repetitions. With continued stress repetitions the modulus increased to approximately the original modulus prior to freeze-thaw. Approximately 10,000 stress repetitions at σ_d = 5 psi and a confining pressure of 2 psi were required to increase the modulus to its original value. McLeod (7) also reported significant decreases in resilient moduli of undisturbed samples of till after one freeze-thaw cycle, and he also reported, based on a very limited number of tests, that the modulus was regained after a number of repeated load applications.

After all the suction and resilient moduli tests were completed on the undisturbed samples, the soil was recombined, and remolded samples were prepared at about the same water content and density. Figure 6 shows the results of the resilient moduli tests on the remolded samples. In order to obtain resilient moduli that are more indicative of the spring value, the remolded samples were put through two cycles of freeze-thaw, and the results are shown in Figure 7. A comparison follows of the resilient moduli obtained for undisturbed samples from the spring and fall samplings with results from remolded samples with and without freeze-thaw. The resilient moduli obtained for the undisturbed samples were 6,300 psi for the spring 1972 sample and 8,200 psi for the fall 1970 sample. The resilient moduli for the remolded samples were 14,800 psi for no freeze-thaw and 6,500 psi for two cycles of freeze-thaw. The water content of the samples was approximately 33 percent. Two cycles of freeze-thaw appear sufficient to condition the samples so that stiffness values similar to those observed in situ are obtained.

SUCTION

During the past several years, numerous researchers have considered the possibility of using soil suction values for pavement design purposes (12, 15). A number of investigators have suggested procedures to measure suction both in the laboratory and in situ. Richards (10) has recommended the use of a psychrometric technique to measure total suction in the field and in the laboratory. Krahn (6) investigated the measurement of total suction by the Richards technique in the laboratory and also the measurement of matrix suction using a modified Anteus Consolidometer as developed by Pufahl (9). The results of these investigations indicate that laboratory techniques appear satisfactory. Field techniques for measuring suction over extended periods of time in cold regions, however, are still in the developmental stage.

Suctions on the Regina-to-Lumsden undisturbed samples before and after freeze-thaw were determined using the Anteus Consolidometer as modified by Pufahl (9). Following these measurements on the undisturbed samples, the soil from all test samples was combined and remolded. Suctions were then determined on remolded and recompacted samples over a range in water contents before and after freeze-thaw.

Results of all the suction tests on Regina clay are shown in Figures 8, 9, and 10. Figure 8 compares suction values on undisturbed and remolded samples prior to freeze-thaw. It is important to note that the undisturbed samples have already been subjected to several freeze-thaw cycles in the field. It is apparent from Figure 8 that the suction values on the undisturbed samples are considerably lower than for the remolded samples. It is difficult to detect a difference in suction values between the fall of 1970 and the spring of 1972. In all cases the undisturbed samples exhibit low suction values. Figure 9 shows suction values for remolded samples before and after freeze-thaw. A very significant drop in suction is evident after the freeze-thaw cycle. Figure 10 shows a comparison of suction values on undisturbed samples before and after freeze-thaw. A small but significant drop in suction occurred on the undisturbed samples after the freeze-thaw cycle. As noted previously, the undisturbed samples ob-

Figure 4. Clay resilient modulus and water content.

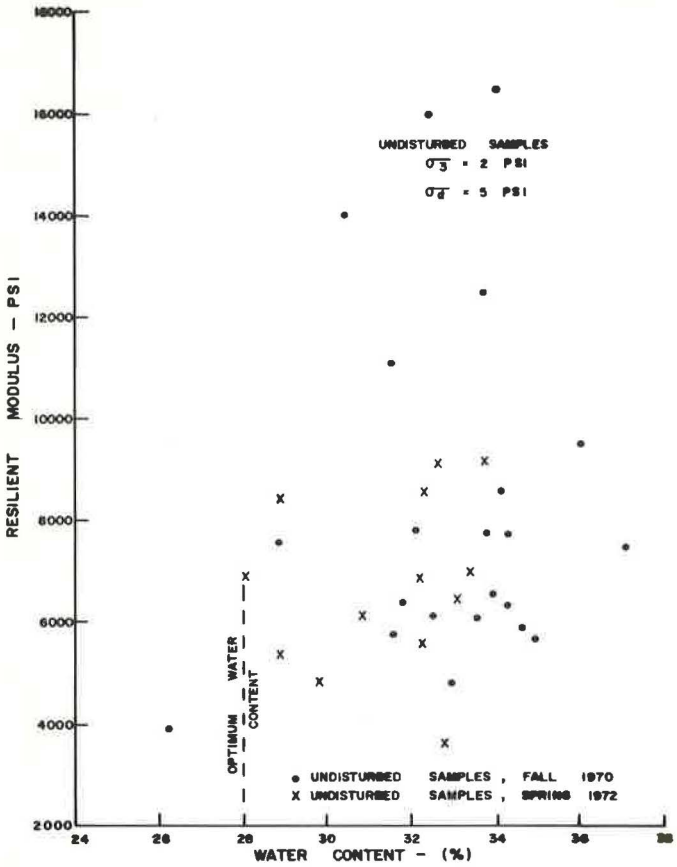

Figure 5. Resilient modulus tests, Regina clay samples, 1970.

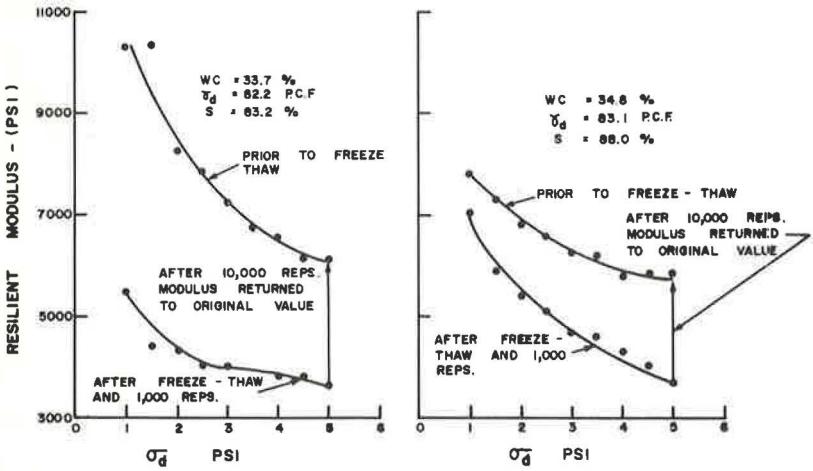

Figure 6. Resilient modulus of subgrade and water content of remolded Regina clay samples (σ_3 = 2 psi and σ_d = 5 psi).

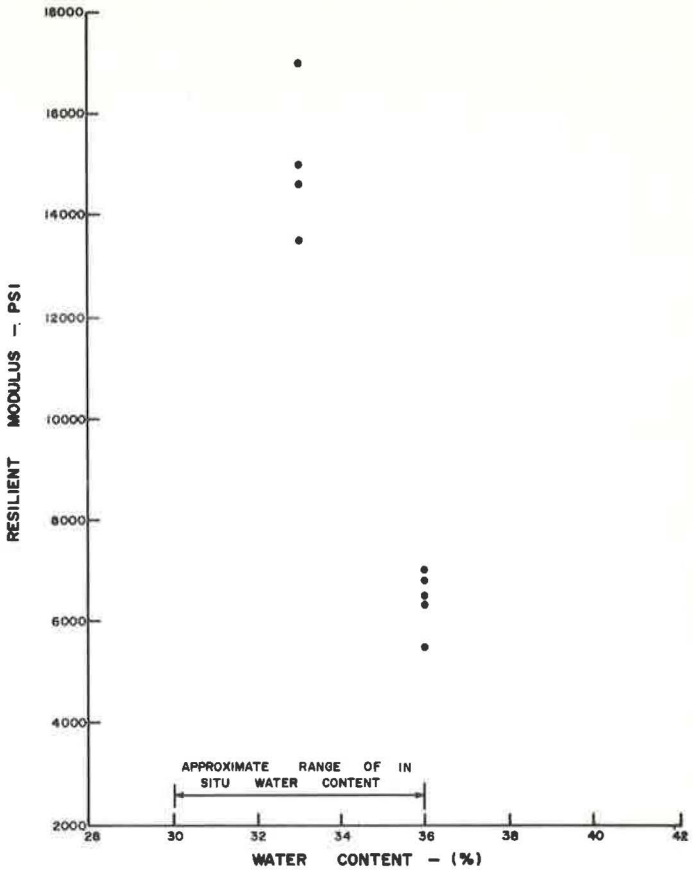

Figure 7. Resilient moduli of remolded samples after two freeze-thaw cycles (σ_3 = 2 psi and σ_d = 5 psi).

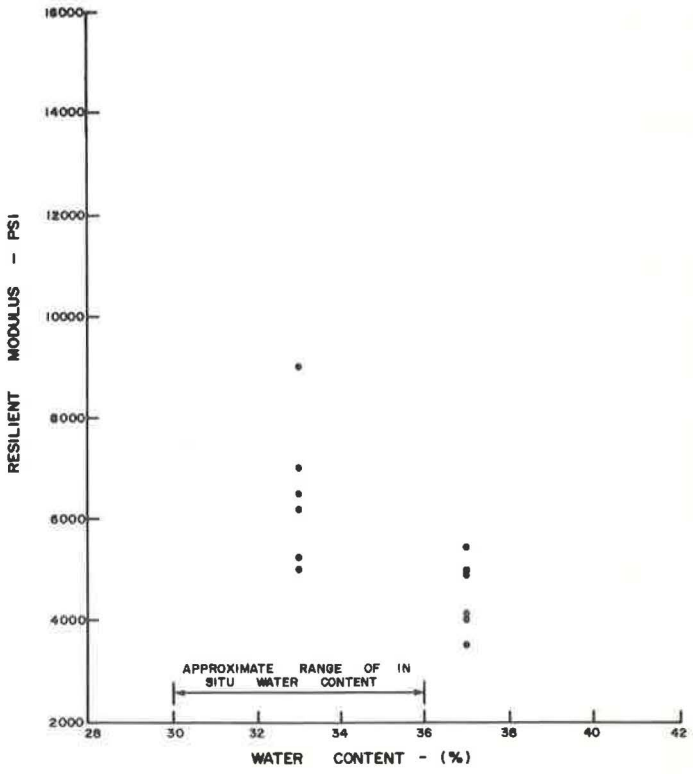

Figure 8. Soil suction values of undisturbed and remolded samples, no freeze-thaw.

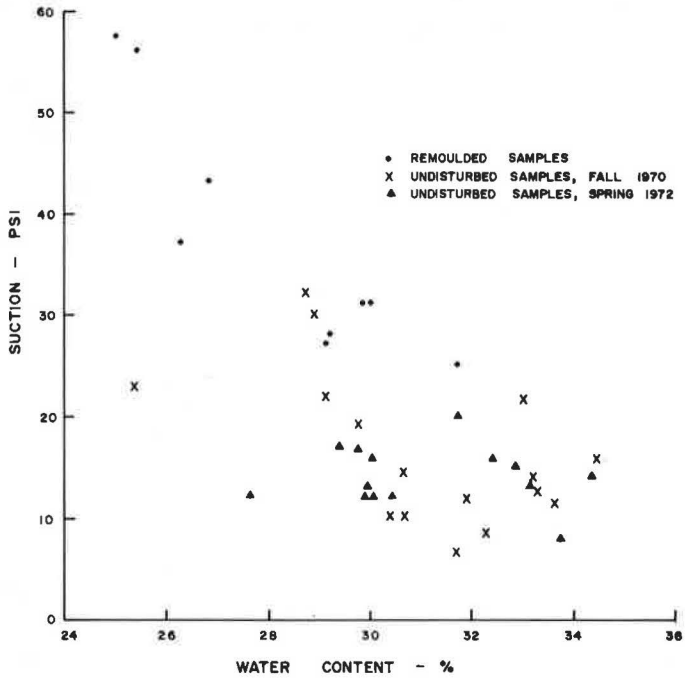

Figure 9. Soil suction values of remolded samples before and after freeze-thaw, fall of 1970.

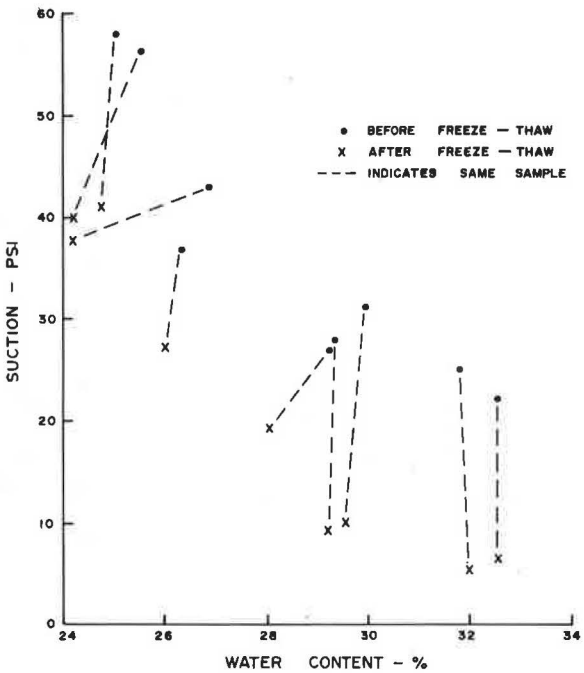

tained during the fall of 1970 have been subjected to several cycles of freeze-thaw, but since the last cycle the roadway has been subjected to considerable truck traffic.

A well-defined secondary structure was present in the undisturbed samples (Fig. 11), and definite ice segregation was evident in the samples as observed by breaking three undisturbed samples in the frozen state. The average suction value of the undisturbed samples of Regina clay was 15 psi. Six of these samples were subjected to one cycle of freeze-thaw, and an average suction of 5 psi was measured after thawing (Fig. 10). This may represent in some way what happens in the subgrade between fall and spring in a cold region.

Mickleborough (8) also did suction tests using a pressure plate device on remolded Regina clay (the same material as tested in this investigation), and found that freeze-thaw cycles reduce suction values (Fig. 12). In this same investigation Mickleborough found that freeze-thaw reduced the resilient modulus by 50 percent at water contents greater than about 28 percent. The possibility of secondary structure affecting the suction was advanced as a possible explanation.

McLeod (7) performed suction tests on undisturbed till samples (Fig. 13) from a subgrade that had been in service for 3 years, and he found similar trends.

A possible explanation for the drop in suction after freeze-thaw is that the water accumulates in the secondary structure during the winter, and then on thawing the free water in the secondary structure controls the suction as measured in the laboratory. During the summer, with repeated stress applications and an internal suction gradient, the moisture is redistributed, and the suction as measured in the laboratory increases.

The suction test results on undisturbed samples from the highway section between Regina and Lumsden and the section of highway studied by McLeod (7) indicate that the suction of undisturbed field samples varies between 5 and 20 psi. It is possible, based on limited freeze-thaw test results, that the maximum suction during the spring is only about 20 psi. In the majority of the cases, the water content was above the standard AASHO optimum and also above the plastic limit. It is apparent that, in order to measure suction in the field, the technique must be precise enough to detect changes in suction in the range between 5 and 50 psi.

Details of a water content study completed during the fall of 1970 at a typical cross section on the Regina-to-Lumsden highway are shown in Figure 14. All water contents are higher than the plastic limit of 29.8 percent and the optimum moisture content of 27.8 percent as determined by the standard AASHO compaction test. A change in water content across the section or with depth is not evident. These data indicate that the suction value in all areas of the roadbed is probably less than 20 psi.

An extensive amount of field work has been carried out to determine the suction under covered areas in regions of moderate temperature. DeBruijn (4) reported a soil suction of 2.8 to 3.8 pF (2 pF = 1.42 psi, 3 pF = 14.2, and 4 pF = 142 psi) under covered areas in South Africa. Richards (10) reported soil suctions between 3 pF and 4 pF in a number of areas studied in Australia. The suction measurements reported (Fig. 8) are much lower than those reported by DeBruijn (4) and Aitchison and Richards (1). Low suction values are difficult to measure in the laboratory and are extremely difficult, if not impossible, to measure in the field with present technology under extremely adverse climatic conditions.

Sauer (11) measured matrix suction under thin pavements (1 in. of asphalt concrete on subgrade) using gypsum blocks during the fall of 1966 in the province of Saskatchewan. Suctions that were measured 2 ft below the pavement on centerline are given in Table 1. Water contents were well below the plastic limit, but still the suction values were very low. Based on work reported on remolded samples (Fig. 9) if the water content for lacustrine clay is 5 percent below the plastic limit the suction should be about 100 psi, but Sauer (11) reported suctions in the order of 10 psi. These observations are in agreement with observed suctions on undisturbed samples from the highway between Regina and Lumsden, as discussed previously. These field observations substantiate the differences found in the laboratory between suction measured on remolded samples and that measured on undisturbed samples.

Figure 10. Soil suction values of undisturbed samples before and after freeze-thaw, fall of 1970.

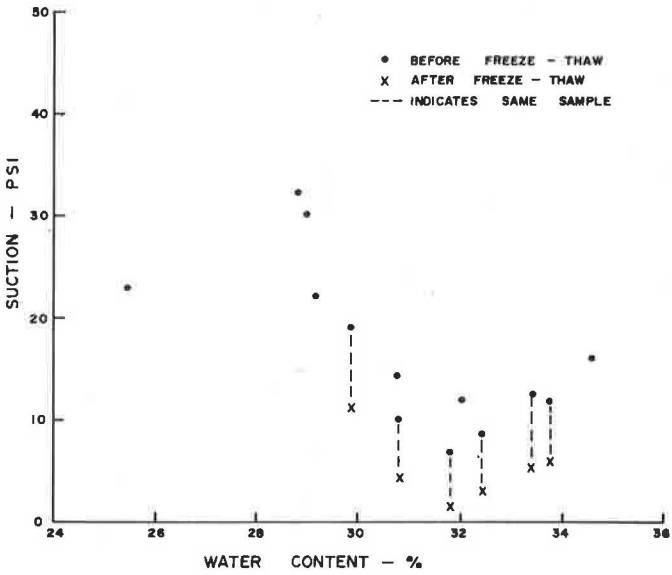

Figure 11. Undisturbed samples of Regina subgrade clay.

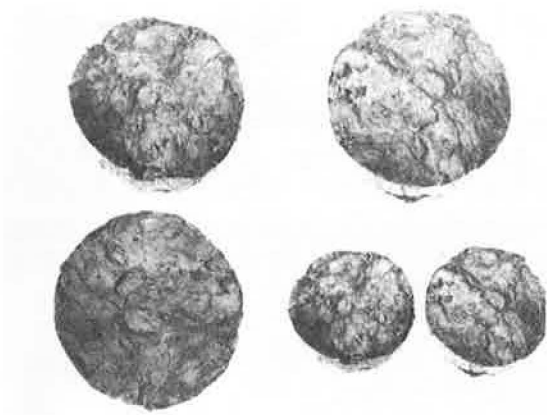

NOTE: Prominent secondary structure in above samples

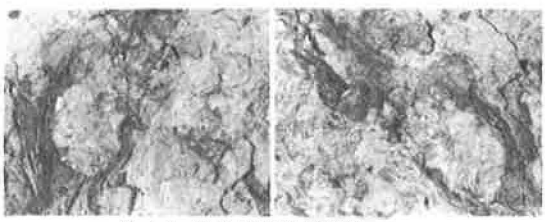

Close-up view of secondary structure

Figure 12. Soil suction and water content of Regina clay.

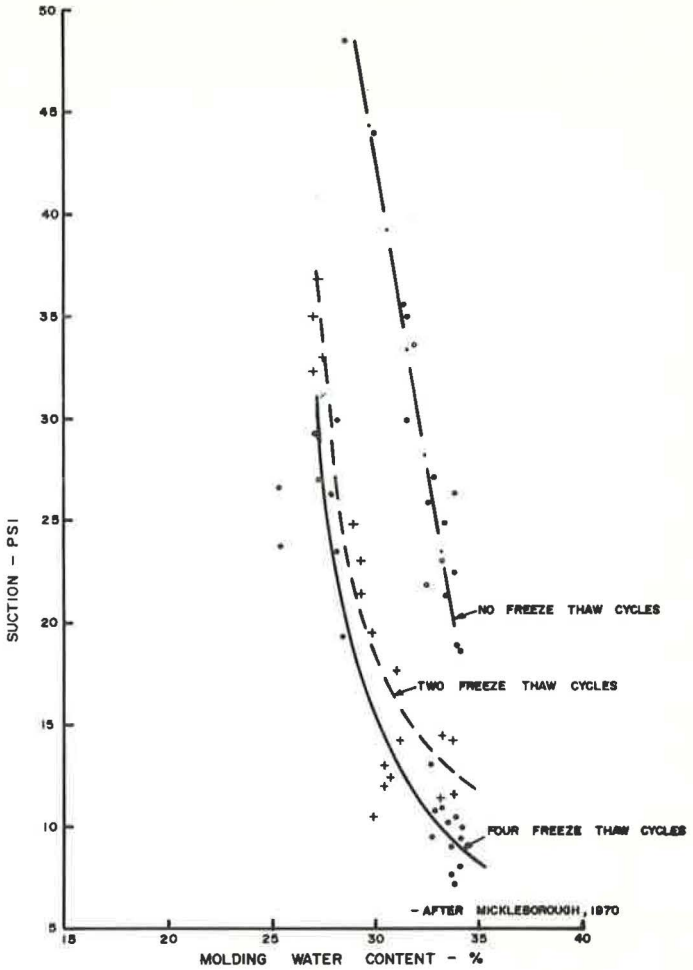

Figure 13. Soil suction and water content of original samples of till subgrade.

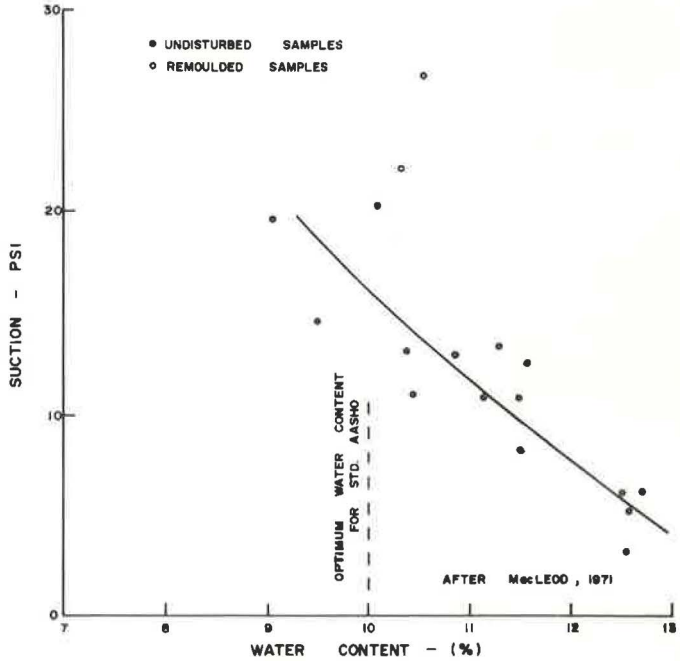

Figure 14. Moisture distribution in the subgrade.

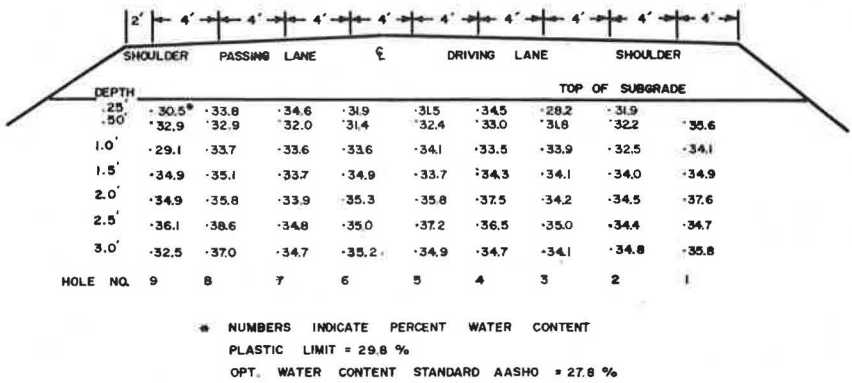

Table 1. Suctions measured by gypsum block (11).

Material	Test Site Number	Suction (psi)	Water Content (percent)	Plastic Limit (percent)
Lacustrine clay	GB-1	10	20	25.5
	GB-9	10	22	25.4
Till	GB-2	13	13	16.8
	GB-4	15	17	11.4
	GB-8	17	18	20.7
	GB-3	2	18	15.6
	GB-7	8	8	16.6
	GB-10	2	10	16.5

Figure 15. Calibration of in situ probes selected at random.

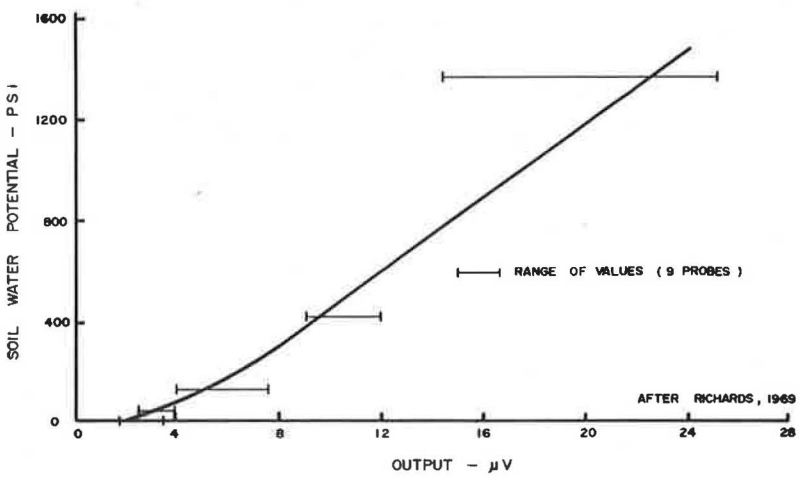

More recently Richards (10) proposed a psychrometric technique for measuring total suction. This type of installation was tried on the section of highway from Regina to Lumsden. The in situ psychrometer was designed and calibrated as outlined by Richards (10). The psychrometers were installed immediately below the outside wheelpath, and psychrometer readings were continued during April, May, and June 1971. The problem in taking such small electrical measurements (μV, microvolt) in the field makes the procedure very sensitive to error. Output readings ranged from 0 to 3 μV with the variation probably caused by measuring problems rather than differences in suction readings. Richards (10) reported the average calibrations for 9 in situ psychrometers as shown in Figure 15. This calibration is almost identical to the calibration of the psychrometers that were installed in the field on the Regina-to-Lumsden section. It is quite easy to see from the calibration why trouble was experienced in trying to detect a suction of about 10 psi or variations between 5 and 20 psi. Richards (10) suggested a psychrometric accuracy of ±15 psi or 25 percent, whichever is greater, but he also suggests that this may be improved somewhat with individual calibration. Krahn (6) used in the laboratory a psychrometer like the one used by Richards (10) and suggested that the psychrometer was not accurate at low suctions. Based on test results and other research presented in the section, the application of a psychrometer to measurement of suction in situ in cold regions does not appear to be sufficiently accurate for the range in suction expected based on findings presented here.

SUMMARY AND CONCLUSIONS

1. In cold regions the resilient modulus of the subgrade exhibits a significant seasonal change.
2. After one freeze-thaw the undisturbed samples decreased significantly in resilient modulus, and after 10,000 applications of load the modulus was regained. It was suggested that behavior reflects what happens in the roadway during spring and summer with repeated truck loading.
3. Testing of remolded samples does not duplicate field conditions in cold regions. For Regina clay, approximately two cycles of freeze-thaw are required to obtain a moduli value indicative of the spring condition.
4. Suctions measured on undisturbed Regina clay were considerably lower than measured suction for remolded Regina clay. It was suggested that this difference could be caused by the development of secondary structure.
5. Field suction values appear to be between 5 and 25 psi for the roads investigated in Saskatchewan. This indicates a need for precise measuring techniques to determine in situ suction values. The psychrometer is not sufficiently accurate for determination of such low suctions.

REFERENCES

1. Aitchison, G. D., and Richards, B. G. A Broad-scale Study of Moisture Conditions in Pavement Subgrade Throughout Australia. In Moisture Equilibria and Moisture Changes in Soils Beneath Covered Areas (Aitchison, G. D., ed.), Butterworths, Inc., Sydney, 1965.
2. Bergan, A. T. Some Considerations in the Design of Asphalt Concrete Pavements for Cold Regions. Univ. of California, Berkeley, PhD dissertation, 1972.
3. Dehlen, G. L. The Effect of Non-Linear Material Response on Behavior of Pavements Subjected to Traffic Loads. Univ. of California, Berkeley, PhD thesis, 1959.
4. DeBruijn, C. M. A. Some Observations on Soil Moisture Conditions Beneath and Adjacent to Tarred Roads and Other Surface Treatments in South Africa. In Moisture Equilibria and Moisture Changes in Soils Beneath Covered Areas (Aitchison, G. D., ed.), Butterworths, Inc., Sydney, 1965.
5. Kasianchuk, D. A. Fatigue Considerations in the Design of Asphalt Concrete Pavements. Univ. of California, Berkeley, PhD thesis, 1968.
6. Krahn, J. Comparison of Soil Pore Water Potential Components. Univ. of Saskatchewan, Saskatoon, MSc thesis, 1970.

7. McLeod, D. R. Some Fatigue Considerations in the Design of Thin Pavements. Univ. of Saskatchewan, Saskatoon, MSc thesis, 1971.
8. Mickleborough, B. W. An Experimental Study of the Effects of Freezing on Clay Subgrades. Univ. of Saskatchewan, Saskatoon, MSc thesis, 1970.
9. Pufahl, D. E. Evaluation of Effective Stress Components in Non-Saturated Soils. Univ. of Saskatchewan, Saskatoon, MSc thesis, 1970.
10. Richards, B. G. Psychrometer Techniques for Measuring Soil Water Potential. Division of Soil Mechanics, Commonwealth Scientific and Industrial Research Organization, Australia, Tech. Rept. 9, 1969.
11. Sauer, E. K. Application of Geotechnical Principles to Road Design Problems. Univ. of California, Berkeley, PhD thesis, 1968.
12. Sauer, E. K., and Monismith, C. L. Influence of Soil Suction on Behavior of a Glacial Till Subjected to Repeated Loading. Highway Research Record 215, 1968, pp. 8-21.
13. Seed, H. B., and Fead, J. W. N. Apparatus for Repeated Loading Tests on Soils. In Papers on Soils—1959 Annual Meeting, ASTM, Philadelphia, STP 254, 1959, pp. 78-87.
14. Monismith, C. L., Epps, J. A., Kasianchuk, D. A., and McLean, D. B. Asphalt Mixture Behavior in Repeated Flexure. Univ. of California, Berkeley, Rept. No. TE70-5, 1971.
15. Richards, B. G., Murphy, H. W., Chan, C. Y. L., and Gordon, R. Preliminary Observations on Soil Moisture and Dry Compaction in Pavement Design on the Darling Downs, Queensland. Proc., Australian Road Research Board, Vol. 5, Pt. 5, 1970, pp. 116-146.

DETERMINATION OF YOUNG'S MODULUS FOR BITUMINOUS MATERIALS IN PAVEMENT DESIGN

S. F. Brown, University of Nottingham, England

The determination of a value of Young's modulus for the bituminous-bound layer of a pavement is an essential part of the use of linear elastic theory in pavement design. Current procedures involve either laboratory testing or the use of the Shell nomographs, neither of which is convenient for routine design calculations. Although it is recognized that temperature is a major factor influencing the in situ modulus of bituminous materials, this paper is concerned primarily with the determination of the other major variable, loading time. Relations were derived for the determination of a representative loading time as a function of vehicle speed and thickness of bituminous layer. This loading time is based on the average pulse time for stresses in the vertical and horizontal directions at various depths in the bituminous layer. Modulus-time-temperature relations for two typical base mixes, of the continuously graded and gap-graded types, were established by modifying Shell nomograph results in the light of a number of experimentally determined values of modulus. A chart was produced from which values of Young's modulus can be determined simply and directly with an accuracy considered adequate for design purposes. An equation was derived that could be used as an alternative to the charts, but its principal purpose is to fit into a computer design program for flexible pavements. The overall objective of this study is to simplify improved design methods with a view to their being more readily acceptable in practice.

•MANY suggestions for improved methods of pavement design using a structural design approach involve analysis of the pavement to determine critical stresses and strains (1, 2, 3). Although various methods of analysis have been used, most require that a value of Young's modulus for the bituminous layer be specified. In structures having a substantial thickness of bituminous-bound material, the characteristics of this layer largely dictate the performance of the pavement. In terms of the analysis, the value of Young's modulus for the bituminous layer has a large influence on the stresses and strains throughout the structure. Hence, a reasonably accurate but straightforward procedure is required for its determination.

Under the dynamic conditions that generally apply to pavement design problems, the bituminous material is assumed to behave elastically. The Young's modulus used in analysis is equated to the stiffness modulus of the material under the applicable conditions of temperature and loading time. When direct measurements are not possible, the most widely used procedure for the determination of stiffness involves using the nomographs developed by the Shell organization (4, 5, 6). The values of stiffness they produce have been shown to correlate reasonably well with other measured values, but their use for practical design is far from convenient. One of the most difficult problems is the specification of a relevant loading time. This arises because of the three-dimensional nature of the structure and of the stresses induced in it by a rolling wheel load.

Sponsored by Committee on Strength and Deformation Characteristics of Pavement Sections.

The object of this paper is to devise a relatively simple method for determining Young's modulus for the bituminous layers in a pavement that will be of sufficient accuracy for routine design purposes. The results are presented in three different ways so that values of modulus may be obtained from plots or tables or by calculation from a single equation that can easily be incorporated in a computer program.

FACTORS INFLUENCING IN SITU YOUNG'S MODULUS

Although flexible pavement construction normally includes more than one layer of bituminous-bound material, the considerations in this paper refer to a single layer only. This approximation is considered adequate when dealing with pavements incorporating bituminous-bound bases because the influence of a different material in the surfacing can be neglected for design purposes, the base being the main structural layer.

In specifying the modulus to be used for a bituminous layer, consideration has to be given to the two factors that influence its magnitude: temperature and loading time.

Temperature

In general, the layer will be subject to a temperature gradient that will depend on the air temperature and the length of time the air has been at that particular temperature. Measurements made by the Transport and Road Research Laboratory reported by Galloway (7) and Forsgate (8) have shown that the pavement temperature, under equilibrium conditions, differs from that of the air. Galloway's measurements indicated that in summer the average temperature of the base and surfacing was slightly above that of the air and that in winter the structure was somewhat below air temperature. This was partially confirmed by Forsgate, though in some structures studied by him pavement temperatures were always above air temperatures even during the winter. His observations, however, were not made below 2 C. Witczak (9) has presented information on average temperatures for pavements of various thicknesses. He showed that the pavement temperature was always above that of the air except for very thin layers at low temperatures. The precise relation between air temperature and pavement temperature depends on many factors, such as exposure to wind, the influence of rain, and surface texture. However, it would seem that the average annual air temperature is likely to be about the same as that for the bituminous layers in the road. In a particular design exercise, such information could be deduced from local meteorological records. Forsgate has shown that this can be done with reasonable accuracy, and Finn et al. (2) have also recommended this procedure. Although loading time is the main subject of this paper, the importance of the influence of temperature on the behavior of asphalt pavements cannot be overemphasized.

Loading Time

Any point in the bituminous layer is subjected to simultaneous variations of stress and strain in three orthogonal directions under the action of a passing wheel load. The amplitude and length of these pulses depend on the direction of action of the particular stress or strain as well as the depth of the point concerned. Hence, no unique loading time exists for the bituminous material in situ.

The definition of loading time used by Van der Poel (4) in establishing the original Shell nomographs was

$$t = \frac{1}{2\pi f} \tag{1}$$

where t = loading time and f = frequency of the sinusoidally applied stress used in the laboratory tests on which the nomograph stiffness values were based. This same definition is used in this paper.

In attempting to define a loading time in connection with the analysis of full-scale trial sections, Klomp and Niesman (10) established two relations: $t = (\frac{1}{2}\pi) \times 0.45$ V

and $t = (\frac{1}{2}\pi) \times 0.3\ V$ for surfacing and bases respectively (where V = vehicle speed in km/hr). These expressions were based on the analysis of measured horizontal strain pulses at various depths in the structures. Some difficulty was encountered in defining exactly the beginning and end of any individual pulse.

This problem was studied further by Hofstra and Valkering (11) in a similar investigation. Measured horizontal strain pulses were again used and the following relation established:

$$t = 0.4d \tag{2}$$

where d = pulse length at half-height.

In both these investigations, the resulting values of Young's modulus, when used in linear elastic analysis of the structures, produced strains that compared favorably with the measured values.

The present aim is to determine a general value of modulus for design use rather than a particular value for computing a particular strain. Hence, the loading time specifications used in these two investigations are not thought to be correct because they are based on only one pulse in one direction, and this does not represent an average loading time for the layer as a whole.

Because the pavement is being subjected to an applied stress regime, the correct loading time is considered to be based on stress pulses rather than strain pulses and should be an average for the three orthogonal stresses: vertical, radial, and tangential. It should also be the mean value for the layer thickness being used because all three pulses increase in length with depth.

DETERMINATION OF LOADING TIME

The development of curves for the determination of pulse loading times to be used in dynamic triaxial testing of paving materials has been described by Barksdale (12). The loading times involved apply only to vertical stresses and for this reason have the same shortcoming as the Shell results discussed in the previous section. However, the method used in developing these curves is based on a combination of theory and experimental observations that form a sound basis for developing the mean loading time required for design purposes.

Barksdale's theoretical analyses indicated that the vertical stress pulse was approximately sinusoidal in shape in the upper part of the pavement. This is the zone of interest in the present investigation and conveniently agrees with the wave shape used in the tests on which the Shell nomographs are based. The definition of loading time used by Barksdale, however, differs from that defined by Van der Poel and is shown in Figure 1. If Barksdale's loading time is t_B, then $f = \frac{1}{2t_B}$, where f = frequency.

Because $f = \frac{1}{2\pi t}$ using Van der Poel's expression,

$$t = \frac{t_B}{\pi} \tag{3}$$

Barksdale took into account inertial and viscous effects in determining his loading times by studying vertical stress pulses measured in the AASHO Road Test. Because of these effects, the length of a particular stress pulse in terms of time will not be proportional to wheel speed.

The theoretical investigation carried out by Barksdale on various structures showed that the vertical stress times were not significantly affected by changes in asphalt stiffness or variations in layer thicknesses. In other words, at any particular depth in a conventional structure, the pulse time is a constant for a given wheel speed.

The curves derived by Barksdale enabled loading time to be determined from depth and vehicle speed and are shown in Figure 2.

In extending this work to deal with stresses in three directions, it has been assumed that the two horizontal stresses will be affected by viscous and inertial effects to the same extent as the vertical stress.

Calculations were performed on two structures in order to determine pulse lengths for vertical, radial, and tangential stresses at various depths. The two structures were chosen to represent constructions with thin and thick bituminous layers, and details are given in Table 1.

The calculations were based on linear elastic layered theory, and the results were obtained using the BISTRO computer program (13). The pulses were produced by plotting each stress against radial distance from the centerline of the single uniformly distributed circular load. This was done at three depths for each structure. The depths were arrived at by dividing the bituminous layer into three equal thicknesses and taking the midpoint of each of these sublayers. The depths were hence one-sixth, one-half, and five-sixths of the thickness of the layer. The object of this was to obtain information that could be used to determine average pulse lengths for the layer as a whole. Examples of some of these pulses are shown in Figure 3. Because of the change from tension to compression, which occurs for horizontal stresses near the center of the layer, the pulses at this depth were not used.

Equivalent pulse lengths were taken off these plots by eye using the same procedure as Barksdale, which involved manually fitting a sine curve to the actual pulse. This procedure avoids the difficulty encountered by Klomp and Neisman (10) of not knowing when the pulse has terminated, because in some cases the stress approaches zero asymptotically.

The next exercise was to establish the relation between the lengths of the two horizontal pulses and that of the vertical pulse. This was done by plotting pulse lengths against depth as shown in Figure 4. A best-fit line was put through the points for each of the three stresses. By taking a mean line for the two horizontal stresses, as shown, it became apparent that the lengths of these pulses were about 1.7 times those of the vertical pulses at any particular depth.

For a given vehicle speed, pulse time is proportional to pulse length. Barksdale's vertical pulse time was denoted by t_s, and the same definition has been used in the preceding analysis. Hence the average pulse time at a particular depth is given by

$$\tfrac{1}{3}(t_s + 1.7t_s + 1.7t_s) \approx 1.5t_s$$

Therefore, the average loading time, using Van der Poel's definition, is

$$t = 1.5t_s/\pi = 0.48t_s$$

Barksdale's corrections for viscous and inertia effects were based on a single AASHO Road Test structure that only contained 125 mm of bituminous-bound material. It was, therefore, necessary to check that the stress pulse depth relations for this structure were similar to those shown in Figure 4 for structures with 300 and 600 mm of bituminous material. Computations similar to those described were carried out, and structural details are given in Table 1. The results are included in Figure 4, and comparison with the other pulse lengths can only be described as fair. Clearly, it would be better if experimental results were available from structures having thicker asphalt layers.

Barksdale's curves were replotted to obtain relations between loading time t and depth for various speeds (Fig. 5). Once the mean loading times were established at various depths for the three stress pulses, it was necessary to determine average loading times for various thicknesses of bituminous layer. This was achieved by changing the abscissas of Figure 5 from depths to layer thicknesses and for each depth taking the average loading time, i.e., the value at half that depth. These modified relations are shown in Figure 5, and it was found that they could be plotted as straight lines.

In converting Barksdale's speeds to the international system of units, odd numbers resulted (Fig. 5). Graphical interpolation on a logarithmic plot enabled round figures to be used (Fig. 6).

Figure 1. Definition of loading time used by Barksdale (12).

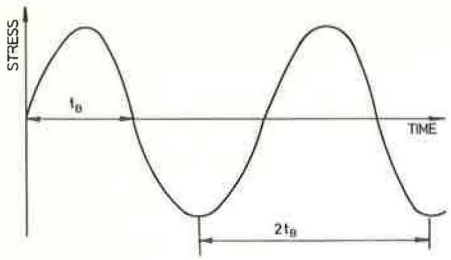

Figure 2. Determination of vertical pulse loading time (after Barksdale, 12).

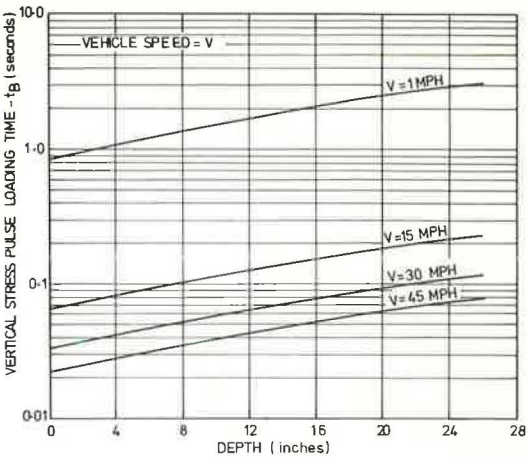

Table 1. Details of structures used for theoretical stress pulse determination.

Layer	Type of Structure	Structure Measure: Modulus $(MN/m)^2$	Poisson's Ratio	Thickness (mm)
Bituminous	Thick	4,000	0.4	600
	Thin	4,000	0.4	300
	AASHO	4,000	0.4	125
Granular base	Thick	—	—	—
	Thin	—	—	—
	AASHO	320	0.3	150
Granular subbase	Thick	125	0.3	150
	Thin	125	0.3	150
	AASHO	125	0.3	300
Subgrade	Thick	50	0.4	—
	Thin	50	0.4	—
	AASHO	50	0.4	—

Note: Load = 40 kN, contact pressure = 500 kN/m^2, and radius of loaded area = 160 mm.

Figure 3. Typical stress pulses in structure with 600-mm bituminous layer.

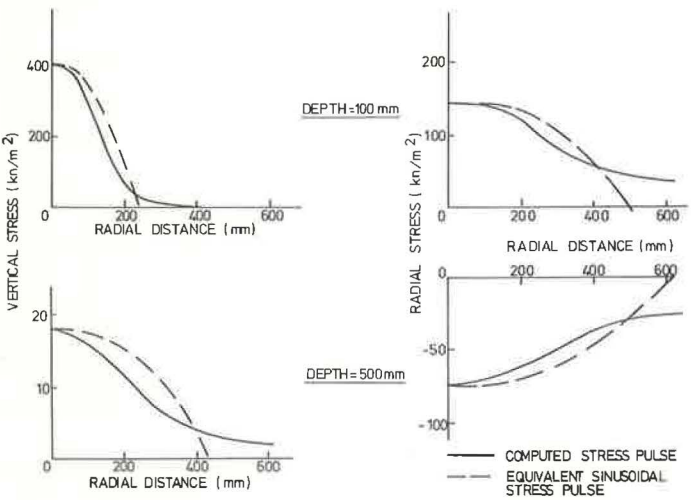

The procedure suggested by Hofstra and Valkering (11) was used to provide results for the purposes of comparison. The loading times in this case were determined from theoretical, horizontal strain pulses at the lowest of the three depths considered for two of the structures detailed in Table 1, excluding the AASHO structure. The calculations were performed at three speeds: 3, 20, and 80 km/hr. The results shown in Figure 6 indicate similar results to those derived from Barksdale's curves but with somewhat shorter loading times. In use, these would lead to higher values of stiffness than the proposed values, which are on the safe side for design purposes.

MODULUS-TIME-TEMPERATURE RELATIONS

This section describes how relations among modulus, loading time, and temperature were derived for two typical types of mix extensively used in flexible pavement construction. A continuously graded mix with a binder having a penetration between 80 and 100 represents a dense bitumen macadam as used in Great Britain and an asphaltic concrete used in the United States. The other mix is of the gap-graded hot-rolled asphalt type used mainly in Great Britain.

In establishing the modulus-time-temperature relations, many of the published results have been studied and compared with values obtained from the Shell nomographs.

Most experimental results are available for the dense bitumen macadam or asphaltic concrete, and many (14-18) have been incorporated in Figure 7. Details of the various tests and the materials used in each case are given in Table 2.

Nomograph values have been calculated for the mix used by Cooper and Pell (14), which was thought to be typical and for which all the details were available. Lines produced from these nomograph stiffnesses for temperatures of 0, 10, and 20 C are shown in Figure 7.

The experimental results shown in Figure 7 were obtained from a variety of tests including direct compression and several types of flexure. The effect of change in modulus between tension and compression was investigated by Kallas (19), but he only reported significant differences at loading times slower than those considered here. The main shortcoming of the selection of results is that all are based on uniaxial stress conditions, whether direct or bending stress, whereas the in situ situation is three-dimensional. Results from triaxial tests with various confining stresses should provide information nearer to this condition, but preliminary results obtained at the University of Nottingham indicate that the confining stress has a relatively small effect on modulus.

By studying flexure and direct compression test results together, a reasonable representation of the in situ situation is obtained because flexural and compressive stresses may be considered analogous to in situ horizontal and vertical stresses respectively.

The results of compression tests by Snaith et al. (16) on dense bitumen macadam and similar tests by Shook and Kallas (15) on asphaltic concrete compare very well for mixes with the same binder content. The beam tests of Epps and Monismith (18) also yield comparable results as do the cantilever tests reported by Freeme (17), though direct comparison is not possible for these latter tests because they were carried out at shorter loading times. The specimens used by Freeme had very high void contents, but by taking the line plotted from nomograph values as a basis for comparison it can be shown that they are only slightly lower than the other experimental results. However, the results reported by Cooper and Pell (14) are significantly lower than the other experimental results.

In deciding on the relations to be used for design purposes, the various experimental points shown in Figure 7 have been used to suggest modifications to the lines based on nomograph values. The resulting straight-line relations are proposed because they reflect the higher measured values of modulus at longer loading times while erring on the low or conservative side (bearing in mind the design applications).

Figure 8 shows the experimental and nomograph values for rolled asphalt. There are fewer experimental points available for this material (17, 18, 20). The high void content of Freeme's mixes produces significantly lower results in this case than for the dense bitumen macadam.

Figure 4. Variation of pulse lengths with depth for various structures.

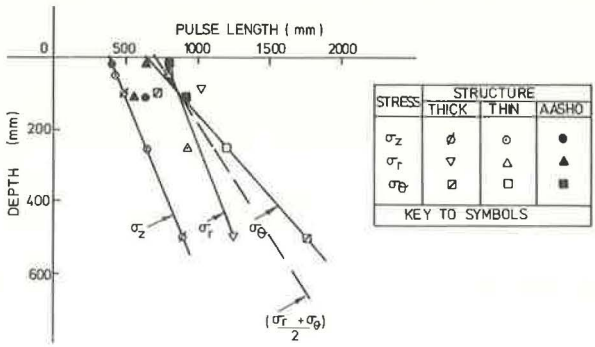

Figure 5. Relation between mean loading time and depth for various vehicle speeds.

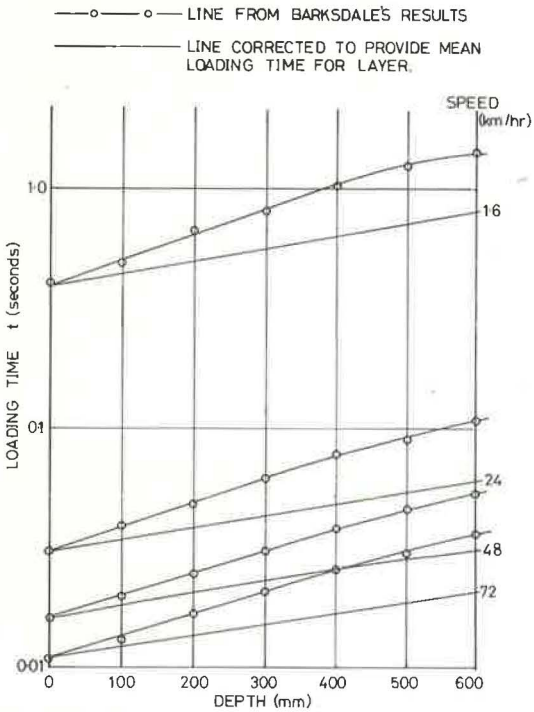

Figure 6. Relation between loading time and thickness of bituminous layer for various vehicle speeds.

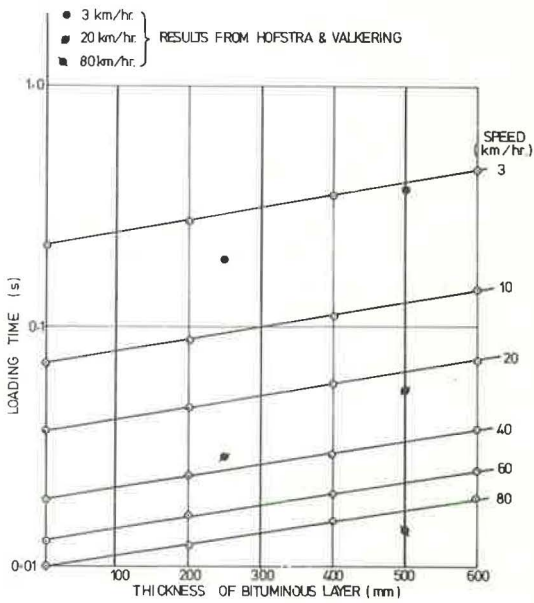

Figure 7. Modulus-time-temperature relation for dense bitumen macadam with 100-penetration binder.

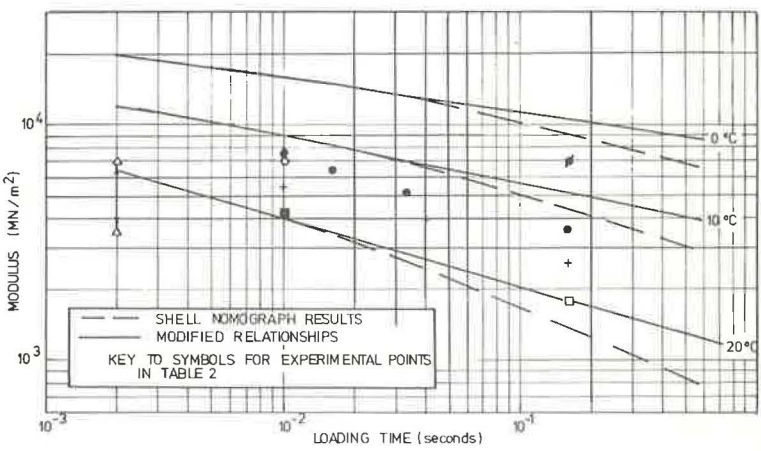

The modified nomograph lines have been established for the rolled asphalt by studying the trends apparent in Figure 7 for the dense bitumen macadam together with the experimental results shown in Figure 8.

An attempt has also been made to carry out the same exercise for a dense bitumen macadam with 200-penetration binder and a dense tar macadam because these materials are also used for base construction in Great Britain. In view of the relatively few experimental results available for these materials, it is difficult to propose any relations with confidence at this time.

GRAPHICAL DETERMINATION OF MODULUS

The previous two sections have described how a representative loading time may be determined from a knowledge of layer thickness and vehicle speed, and this loading time may be used together with the temperature to determine the required Young's modulus.

By combining Figure 6 with Figure 7 or 8, a single chart results from which modulus may be determined directly. This arises because loading time is common to all plots. Figure 9 shows such a combined plot for the dense bitumen macadam with 100-penetration binder.

The advantage of this chart is that it affords the designer a quick method of determining Young's modulus from the design parameters that he is able to specify. At the outset of a design exercise, an estimate has to be made of the thickness of bituminous material. This can be modified subsequently if it is significantly at variance with the final thickness obtained from the design calculations.

Although interpolated values can be estimated from the chart, extrapolation beyond the limits plotted is not likely to be accurate in view of the procedures used to establish the relations.

The dotted line shown in Figure 9 indicates, by way of example, that, for a 275-mm layer at 10 C, the modulus is 7,500 MN/m^2.

EQUATIONS FOR CALCULATION OF MODULUS

All of the plotted lines shown in Figure 9, together with the other modulus-loading time-temperature relations shown in Figure 8, are straight lines on either logarithmic or semilogarithmic scales. It was thus a relatively simple exercise to determine equations to fit all of the plotted lines.

The relation among loading time (t), layer thickness (h), and vehicle speed (V) (Figs. 6 and 9) is as follows:

$$\log_{10}t = 0.5h - 0.2 - 0.94\log_{10}V \tag{4}$$

where t is in seconds, h is in meters, and V is in km/hr.

The expressions derived for the two sets of modulus-time-temperature relations were of the following form:

$$\log_{10}E = \log_{10}(aT^2 - bT + c) - 10^{-4}(dT^2 + eT + f)\log_{10}t \tag{5}$$

where E = Young's modulus in MN/m^2, T = temperature in C, and a, b, c, d, e, and f are constants that depend on the material. When the preceding expressions are combined to eliminate loading time the following equation results:

$$\log_{10}E = \log_{10}(aT^2 - bT + c) - 10^{-4}(dT^2 + eT + f)(0.5h - 0.2 - 0.94\log_{10}V) \tag{6}$$

Values of the constants for the two materials investigated are given in Table 3.

Using this equation, values of modulus have been calculated for a range of values of the three basic variables: temperature, layer thickness, and vehicle speed. Figure 10 shows the results produced using a simple computer program.

One of the main advantages in establishing an equation for the determination of Young's modulus for the bituminous layer of a pavement structure is that it may be incorporated in a computer program to perform the pavement design calculations.

Table 2. Mix details of 100-penetration binder macadams and asphalt concrete and 45-penetration binder rolled asphalt.

Investigator	Material	Type of Test	Binder Content (percent)	Void Content (percent)	Temperature (C)	Symbol Used in Figures
Snaith et al.	Dense bitumen macadam	Compression	4	5	10	◐
Cooper and Pell	Dense bitumen macadam	Flexure of cantilever	6	3	10	○
Snaith et al.	Dense bitumen macadam	Compression	4	5	20	●
Epps and Monismith	Asphaltic concrete	Flexure of beam	6	6	20	□
Shook and Kallas	Asphaltic concrete	Compression	4	6	20	◆
Shook and Kallas	Asphaltic concrete	Compression	5	6	20	+
Shook and Kallas	Asphaltic concrete	Compression	6	6	20	■
Freeme	Dense bitumen macadam	Flexure of cantilever	5 to 6	6 to 12	20	△
Taylor	Rolled asphalt	Flexure of cantilever	6	5	0	◐
Taylor	Rolled asphalt	Flexure of cantilever	6	5	10	○
Taylor	Rolled asphalt	Flexure of cantilever	6	5	20	◔
Freeme	Rolled asphalt	Flexure of cantilever	6	13 to 20	20	△
Epps and Monismith	Rolled asphalt	Flexure of beam	8	6	20	□

Figure 8. Modulus-time-temperature relation for rolled asphalt.

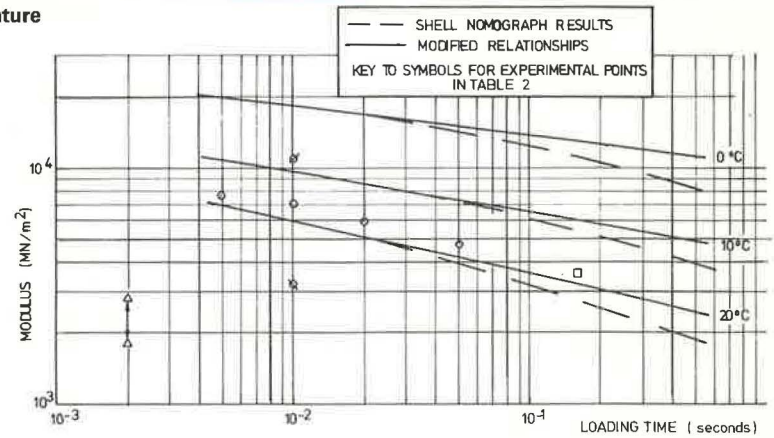

Figure 9. Chart for determination of Young's modulus for dense bitumen macadam with 100-penetration binder.

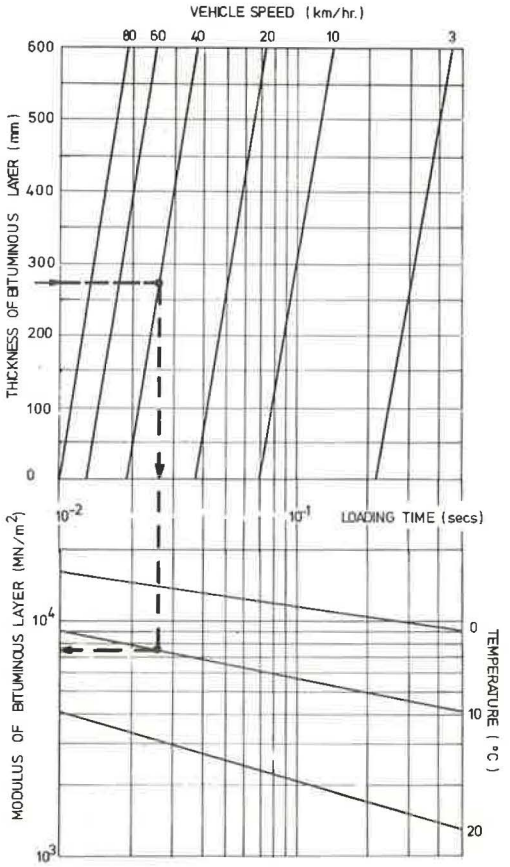

Table 3. Constants for determining Young's modulus (using Eq. 6).

Material	Constant					
	a	b	c	d	e	f
Dense bitumen macadam	10.2	557	8,120	1.8	36.0	1,470
Rolled asphalt	20.2	793	10,360	0	51.5	1,200

Figure 10. Printout of Young's modulus values (computed from Eq. 6).

MATERIAL = D.B.M.100 TEMPERATURE = 15 DEG C ELASTIC MODULI = MN PER SQUARE METRE

H METRES	V KM PER HOUR								
	3	6	10	15	20	30	40	60	80
0.100	2873	3363	3776	4140	4420	4846	5173	5672	6054
0.125	2853	3339	3750	4112	4389	4812	5137	5632	6013
0.150	2833	3316	3724	4083	4359	4779	5101	5593	5971
0.175	2814	3293	3698	4055	4328	4746	5066	5555	5930
0.200	2794	3270	3673	4027	4298	4713	5031	5516	5888
0.225	2775	3248	3647	3999	4269	4680	4996	5478	5848
0.250	2754	3225	3622	3971	4239	4648	4962	5440	5807
0.275	2736	3203	3597	3944	4210	4616	4927	5402	5767
0.300	2718	3184	3572	3916	4181	4584	4893	5365	5727
0.325	2699	3159	3547	3889	4152	4552	4859	5328	5687
0.350	2680	3137	3523	3862	4123	4520	4826	5291	5648
0.375	2661	3115	3498	3835	4094	4489	4792	5254	5609
0.400	2643	3093	3474	3809	4066	4458	4759	5218	5570
0.425	2625	3072	3450	3782	4038	4427	4726	5182	5531
0.450	2606	3051	3426	3756	4010	4398	4693	5146	5493
0.475	2588	3030	3402	3730	3982	4366	4661	5110	5455
0.500	2571	3009	3379	3704	3954	4336	4628	5075	5417
0.525	2553	2988	3355	3679	3927	4306	4596	5040	5380
0.550	2535	2967	3332	3653	3900	4276	4564	5005	5342
0.575	2517	2947	3309	3628	3873	4246	4533	4970	5305
0.600	2500	2926	3286	3603	3846	4217	4501	4936	5269

Brown (21) has described a computer program called Interpolation, which performs an adequate linear elastic analysis of three-layered structures for design purposes. This program has already been incorporated in a simplified pavement design program. Using the procedure described by Brown and Pell (1) should make it much easier to perform structural design calculations either semimanually or completely by computer.

SUMMARY

In previous publications (1, 21), the author has attempted to present, in a simplified manner, the procedures necessary to design a flexible pavement using the structural design approach. The aim has been to bridge the gap between the very complex procedures being discussed at research level and the empirical rules largely used in practice. The results of the vast amount of research in many countries aimed at developing this improved method of design will only find their way into practice if they are presented in a straightforward manner and in a way that design engineers can use.

The digital computer has become a firmly established tool for civil engineers, and its use is essential to the improvement of pavement design procedures. Nonetheless computing time is expensive, and therefore design calculations need to be as simple as possible yet accurate.

This paper has not considered a number of detailed considerations in order to present something of use to pavement designers. For instance, it is well known that the stiffness of a particular material at a certain temperature and loading time is influenced by mix details such as binder content and filler content. More importantly, the degree of compaction strongly influences stiffness by controlling the void content. The relations presented in this paper are thought to represent the characteristics of the two mixes when well compacted to produce void contents of 6 percent or better.

ACKNOWLEDGMENTS

The author wishes to express his thanks to R. C. Coates, University of Nottingham, for providing the facilities necessary for this investigation and to P. S. Pell for several helpful discussions. The computer programming was done by P. Ansell.

REFERENCES

1. Brown, S. F., and Pell, P. S. A Fundamental Structural Design Procedure for Flexible Pavements. Proc. 3rd Internat. Conf. on the Struct. Design of Asphalt Pavements, London, 1972, pp. 369-381.
2. Finn, F. N., Nair, K., and Monismith, C. L. Applications of Theory in the Design of Asphalt Pavements. Proc. 3rd Internat. Conf. on the Struct. Design of Asphalt Pavements, London, 1972, pp. 392-409.
3. Dormon, G. M., and Metcalf, C. T. Design Curves for Flexible Pavements Based on Layered System Theory. Highway Research Record 71, 1965, pp. 69-84.
4. Van der Poel, C. A General System Describing the Visco-Elastic Properties of Bitumens and Its Relation to Routine Test Data. Jour. of Appl. Chem., Vol. 4, 1954, pp. 221-236.
5. Heukelom, W., and Klomp, A. J. G. Road Design and Dynamic Loading. Proc. AAPT, Vol. 33, 1964.
6. Van Draat, W. E. F., and Sommer, P. Ein Gerät zur Bestimmung der dynamischen Elastizitätsmodulu von Asphalt. Strasse und Autobahn, Vol. 6, 1965.
7. Galloway, J. W. Temperature Durations at Various Depths in Bituminous Roads. TRRL Rept. LR 138, 1968.
8. Forsgate, J. Temperature Frequency Distributions in Flexible Road Pavements. TRRL Rept. LR 438, 1972.
9. Witczak, M. W. Design of Full-Depth Asphalt Airfield Pavements. Proc. 3rd Internat. Conf. on the Struct. Design of Asphalt Pavements, London, 1972, pp. 550-567.
10. Klomp, A. J. G., and Niesman, T. W. Observed and Calculated Strains at Various Depths in Asphalt Pavements. Proc. 2nd Internat. Conf. on the Struct. Design of Asphalt Pavements, 1967, pp. 671-688.

11. Hofstra, A., and Valkering, C. P. The Modulus of Asphalt Layers at High Temperatures: Comparison of Laboratory Measurements Under Simulated Traffic Conditions With Theory. Proc. 3rd Internat. Conf. on the Struct. Design of Asphalt Pavements, London, 1972, pp. 430-443.
12. Barksdale, R. G. Compressive Stress Pulse Times in Flexible Pavements for Use in Dynamic Testing. Highway Research Record 345, 1971, pp. 32-44.
13. Peutz, M. G. F., van Kempen, H. P. M., and Jones, A. Layered Systems Under Normal Surface Loads. Highway Research Record 228, 1968, pp. 34-45.
14. Cooper, K. E., and Pell, P. S. Fatigue Properties of Bituminous Road Materials. Univ. of Nottingham, Res. Rept., 1972.
15. Shook, J. F., and Kallas, B. F. Factors Influencing Dynamic Modulus of Asphalt Concrete. Proc. AAPT, Vol. 38, 1969, pp. 140-166.
16. Snaith, M. S., Brown, S. F., and Pell, P. S. Permanent Deformation of Flexible Paving Materials. Univ. of Nottingham, Res. Rept., 1972.
17. Freeme, C. R. Fatigue Properties of Bituminous Mixes. Nat. Inst. for Road Research, C.S.I.R., S. Africa, Internal Rept. RB/4/71, 1971.
18. Epps, J. A., and Monismith, C. L. Influence of Mixture Variables on the Flexural Fatigue Properties of Asphalt Concrete. Proc. AAPT, Vol. 38, 1969, pp. 423-464.
19. Kallas, B. F. Dynamic Modulus of Asphalt Concrete in Tension and Tension-Compression. Proc. AAPT, Vol. 39, 1970, pp. 1-20.
20. Taylor, I. F. Asphaltic Road Materials in Fatigue. Univ. of Nottingham, PhD thesis, 1968.
21. Brown, S. F. Computation of Stresses and Strains for the Design of Flexible Pavements. Highway Research Record 407, 1972, pp. 55-64.

GRAPHICAL TECHNIQUE FOR DETERMINING THE ELASTIC MODULI OF A TWO-LAYER STRUCTURE FROM MEASURED SURFACE DEFLECTIONS

Gilbert Swift, Texas Transportation Institute, Texas A&M University

ABRIDGMENT

•DEFLECTIONS measured on the surface of pavement structures have been seen to resemble deflections computed for layered elastic systems. Accordingly, it becomes desirable to ascertain what theoretical elastic structure most closely resembles a given pavement structure with respect to its deflections. The elastic moduli of the layers in this theoretical structure can then be applied to characterize the materials in the pavement structure and used to compare one structure with another in terms of elastic theory.

The equations of elasticity permit calculation of deflections, given the elastic properties and the thickness of each layer. However, the reverse problem, that of determining the elastic properties of a layered structure from knowledge of its deflections, is not amenable to direct analytic solution. Indirect methods, such as the graphical technique described here, are therefore required to solve this problem. The mathematical basis for this method is discussed elsewhere (1). A computer program that permits finding the elastic moduli of a two-layer structure from the deflections observed at two locations on its surface has been described by Scrivner, Michalak, and Moore (2). In contrast to that method, the technique presented here utilizes the deflections at any plurality of locations.

Use of Figure 1 permits rapid comparisons to be made between surface deflection measurements and deflections computed in accordance with two-layer elastic theory (3). Using a set of five deflection measurements, such as is normally obtained with the Dynaflect (4), together with knowledge or an estimate of the thickness of the upper layer, one can analyze a wide range of structures without encountering non-unique solutions. Within less than a minute after a set of deflections has been measured, one can determine from Figure 1 whether these measurements correspond to an elastic system having a single layer (homogeneous) or two or more layers; whenever the number of layers is two or less, one can also determine the modulus values required by the theory of elasticity to account for the observed deflections.

Deflections observed at several locations can be compared by using the figure to determine whether it is the deep or shallow material at a given location that causes the deflections to differ from those at another location.

USE OF FIGURE 1

In order to use Figure 1, values of the quantity wr/P derived from the measured deflection data are plotted versus r on a separate sheet of bilogarithmic graph paper whose scales match those of the chart, or on a tracing paper overlay. Here w represents the vertical deflection (inches) observed at a distance, r (inches), from the load, P (pounds), applied at a point, or on an area having dimensions that are small compared with r. For Dynaflect measurements, evaluating the quantity wr/P merely requires multiplying the deflections measured at the five standard locations by 10, 15.6,

Sponsored by Committee on Strength and Deformation Characteristics of Pavement Sections.

26, 37.4, and 49 in. respectively. The resulting values (wr per 1,000 lb) are then used to plot the set of points on the separate sheet. The plot is then superimposed on Figure 1 and aligned such that the vertical line r/h = 1.0 of the chart coincides with the vertical line of the plot, for which r is equal to the known or assumed layer thickness, h. Next the plot is shifted vertically, while the alignment is maintained, until the set of plotted points coincides with one or fits well between two of the curves of the figure.

The ratio E_1/E_2 is then obtained, either directly from the identification on the one curve or by interpolation between those of two adjacent curves. The value of E_2, in psi, is obtained by observing where the horizontal line of the plot corresponding to wr/P = 0.01 in.^{2}/1,000 lb intersects the numerical scale [of the quantity 10^5 (wrE_2/P)] on the figure. Finally, the value of E_1 is obtained by multiplying E_2 by E_1/E_2.

PLOT EXAMPLES

Figure 2 shows the three examples of plots made on tracing paper that was superimposed over a bilogarithmic grid (Fig. 3) having dimensions equal to those of Figure 1. These plots are shown as they would appear when aligned for best fit with the chart, but for clarity only a portion of the numerical scale and the line r/h = 1.0 of the chart are shown.

Figure 2 shows how Figure 1 is used to interpret deflections measured at the same location at three different stages of construction. The deflections from which Figure 2a was plotted were obtained on an excavated natural clay foundation. A close fit is found to the theoretical curve for $E_1/E_2 = 1/5$ (from which E_1/E_2 is estimated equal to $1/5.3$), at h = 24 in., and the value for E_2 is found to be 24,000 psi. These results indicate that the upper 2 ft of this foundation material has a substantially lower modulus ($E_1 \approx 4{,}500$ psi) than the deeper material.

After compaction of a 2-ft thick layer of sandy clay fill on this foundation, the deflection data were used to obtain the plots shown in Figure 2b. This plot fits the chart at h = 48 in., $E_1/E_2 \approx 1/2.2$, and E_2 = 26,000 psi ($E_1 \approx 11{,}800$ psi).

Finally, on completion of 3 ft of the sandy clay fill and construction of an 18-in. thick stabilized limestone base course, the deflections plotted in Figure 2c were observed. This plot, when fitted to the chart at h = 18 in. gives $E_1/E_2 \approx 20$ and E_2 = 26,000 psi (E_1 = 520,000 psi).

SPECIAL CASES AND LIMITATIONS

If the modulus of the upper layer is substantially less than that of the lower layer, the best fit of the plotted points may sometimes require a horizontal shift of the plot with respect to Figure 1. In such cases, a value for the layer thickness can be obtained from the figure by shifting the plot to secure the best fit and noting the value of r on the plot, which then coincides with the line r/h = 1.0 of the figure. The value of h is obtained at once from the relation h = r.

In other cases, in which the ratio E_1/E_2 and the layer thickness, h, are both large, multiple solutions (equally good fits between the plotted points and several different curves of the figure) will be obtained unless h is specified and unless at least one of the deflection measurements has been made at a sufficiently great distance from the load. Any such need for additional data becomes apparent as soon as the plot is aligned with Figure 1.

In some instances the measured deflections may give rise to a set of plotted points that fails to conform with any of the curves of Figure 1. It is likely that these instances represent data from structures having more than two layers. Although the method presented here can be extended to include three-layer cases, by calculating and plotting the requisite set of figures, this has not yet been done extensively. However, the presence and the general character of a third layer can often be recognized by observing the shape of the line formed by the plotted points. A strongly convex upward shape, for example, corresponds to the presence of an intermediate layer, the modulus of which is smaller than the moduli of the other two layers.

Although the present figure has been constructed for the specific case of Poisson's ratio equal to 0.5 in both layers, this is believed to represent only a minor limitation.

Figure 1. Two-layer elastic deflection chart (Poisson's ratio, $\sigma = 0.5$).

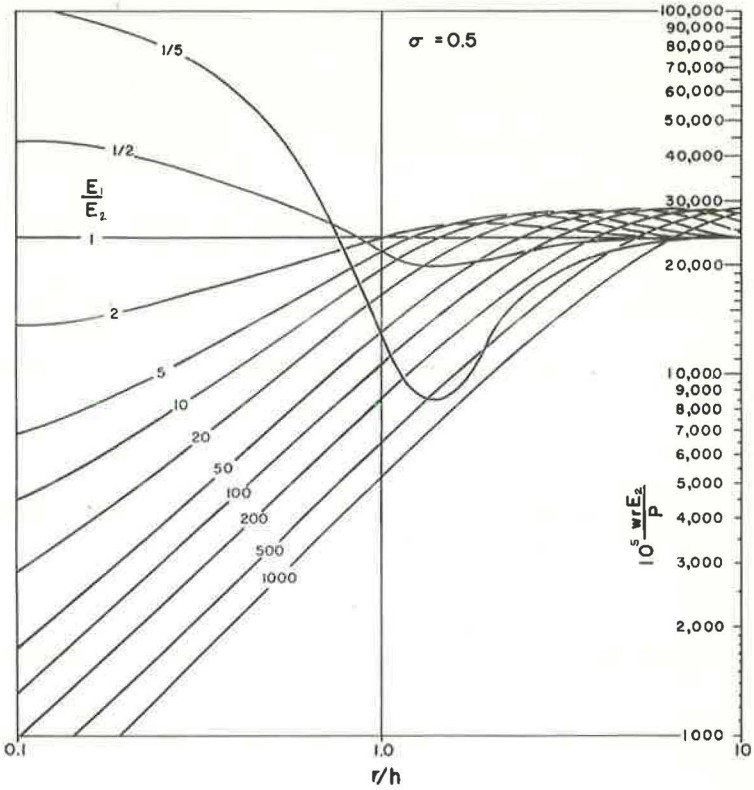

Figure 2. Deflection data from three stages of construction (plotted over grid shown in Fig. 3 and fitted to Fig. 1).

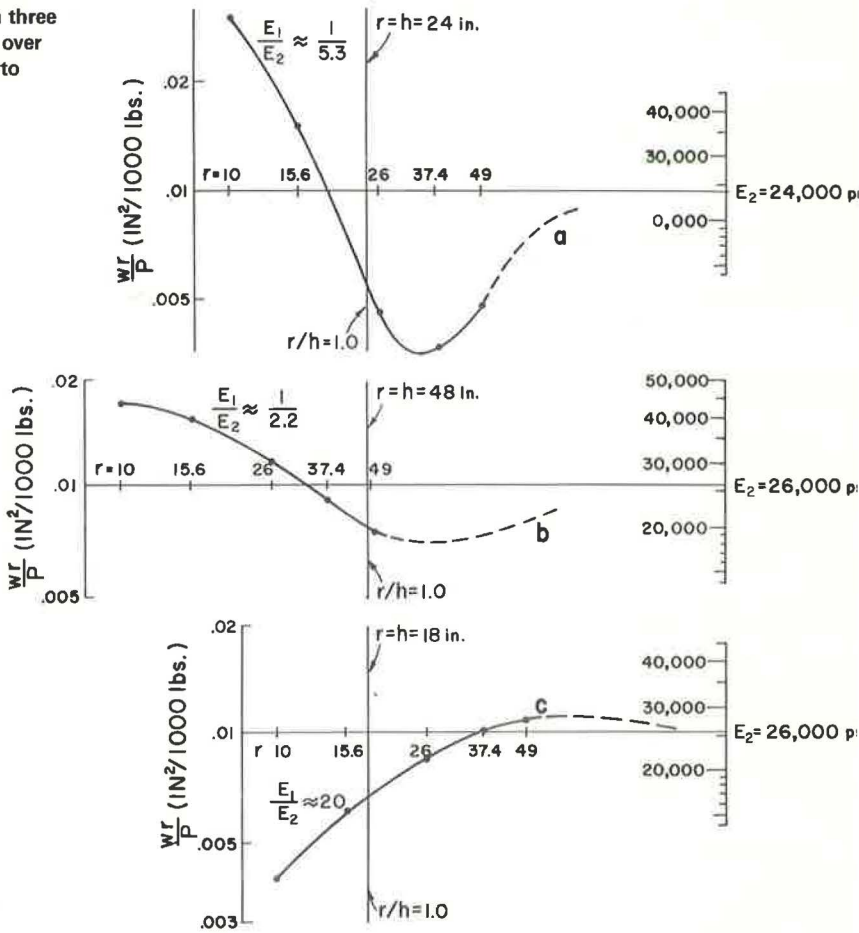

Figure 3. Bilogarithmic grid, dimensionally equal to Figure 1.

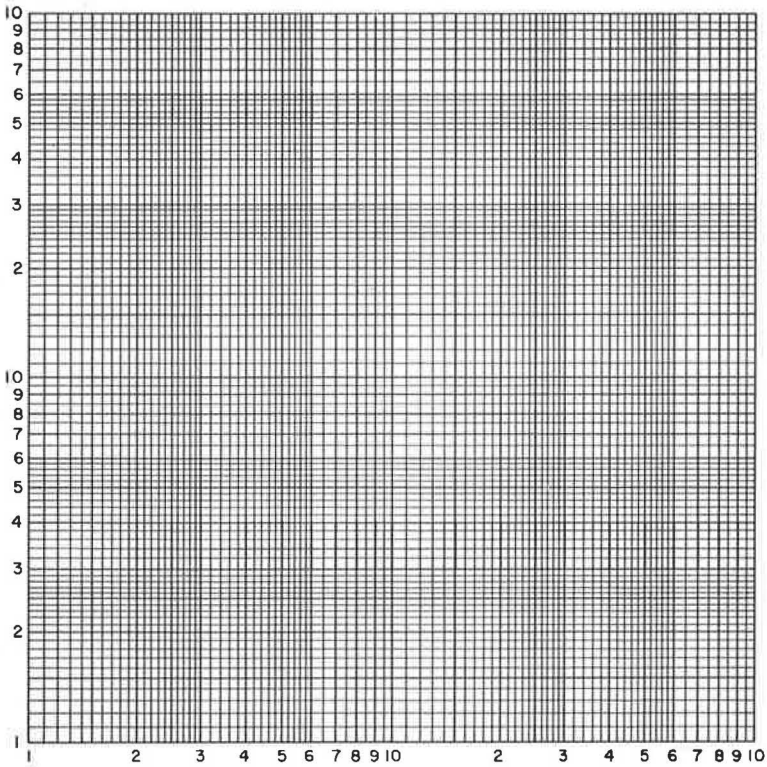

Similar figures could be constructed for other values of Poisson's ratio, but the moduli determined from them, using a given set of deflection data, would not differ greatly. For example, a figure based on Poisson's ratio equal to 0.25 instead of 0.5 would generally provide values for the moduli approximately 20 percent smaller.

CONCLUSIONS

The following conclusions are supported by the study results:

1. A figure has been designed by means of which a set of observed surface deflection data can be compared rapidly against deflections computed in accordance with two-layer elastic theory.
2. The chart can be used to indicate whether a given set of deflections corresponds to an elastic system having one layer (homogeneous) or two or more layers. In the homogeneous and two-layer cases, it provides a means for determining the modulus values required by the theory of elasticity to account for the observed deflections.
3. In certain specific cases, the figure can be used to determine the layer thickness in addition to the moduli, but more generally the layer thickness must be specified to obtain unique values for the two moduli.
4. Extension of the technique to more than two layers is feasible.

ACKNOWLEDGMENT

This research was done by the Texas Transportation Institute, Texas A&M University, in cooperation with the Texas Highway Department and the Federal Highway Administration. The author wishes to thank all members of the Institute who assisted in the work leading to the present report, especially F. H. Scrivner and W. M. Moore who provided valuable assistance and advice in connection with the mathematical phases and C. E. Schlieker who drew the final version of Figure 1. The author is grateful to the Texas Highway Department and especially to James L. Brown and L. J. Buttler for their support of this research.

The contents of this paper reflect the views of the author who is responsible for the facts and the accuracy of the data presented here. The contents do not necessarily reflect the official views or policies of the Federal Highway Administration. This paper does not constitute a standard, specification, or regulation.

REFERENCES

1. Swift, G. A Graphical Technique for Determining the Elastic Moduli of a Two-Layered Structure From Measured Surface Deflections. Texas Transportation Institute, Texas A&M Univ., College Station, Res. Rept. 136-3, Nov. 1972.
2. Scrivner, F. H., Michalak, C. H., and Moore, W. M. Calculation of the Elastic Moduli of a Two-Layer Pavement System From Measured Surface Deflections. Published in this Record.
3. Burmister, D. M. The Theory of Stresses and Displacements in Layered Systems and Applications to the Design of Airport Runways. HRB Proc., Vol. 23, 1943, p. 130.
4. Scrivner, F. H., Swift, G., and Moore, W. M. A New Research Tool for Measuring Pavement Deflection. Highway Research Record 129, 1966, pp. 1-11.

PERMEABILITY COEFFICIENT USING A NEW PLASTIC DEVICE

Joseph E. Bowles, Department of Civil Engineering, Bradley University

The value of the coefficient of permeability of several granular materials determined with the widely used metal compaction mold from the standard compaction test is compared to a plastic device developed by the author. In general, the plastic device provides values 2 to 9 times larger than does the metal mold. If the coefficient of permeability, k, of the porous stone used in the metal mold is separately determined and k-values adjusted for a two-layer system, the plastic mold provides values about 2 to 3 times larger.

•THE metal compaction mold shown in Figure 1 is widely used to determine the coefficient of permeability of most soils. This is in spite of the several permeability devices reported by others (2, 3, 4). The use of the metal mold is of questionable validity, however, for both cohesive (and relatively impermeable) and granular soils. The advantage of using the compaction mold for cohesive soils is that one can compact a specimen to some density, then interchange the base of the standard compaction cylinder with the permeameter base that contains a porous stone and drainage outlet, and then add the top that contains a water inlet and air bleed valve. For granular soils, one simply fills the mold in several layers. Various densities can be achieved by using a noncommercial rod, to which a 9.8-cm diameter plate has been attached, and a rubber mallet (1) (Fig. 2). By inserting the plate into the partly filled mold and applying pressure while simultaneously rapping the sides of the mold with the mallet, one can obtain some rearrangement of soil grains and change in density.

A discussion of the determination of k for cohesive soils is beyond the scope of this paper (except to point out that, for small values of k, it is mandatory to use a thin sample, say, less than 3 cm thick). For $k = 1 \times 10^{-3}$ cm/min and a constant hydraulic gradient of i = h/L of 30, the time for a drop of water to travel through a 3-cm sample is about

$$T = 3/(30 \times 10^{-3}) = 100 \text{ min}$$

For an 11.6-cm mold, the time is about 390 min, or approximately 6½ hours. Without special precautions, sample drainage or evaporation may take place during this length of time. Either of these factors will of course invalidate the test results. This means it is almost mandatory to use a consolidation test setup to determine the coefficient of permeability of cohesive soils.

Saturation, without entrapping air, is a problem with the metal compaction mold. The most efficient method (1) is to submerge the airtight system into a container of water and allow water to back up through the exit tube until water stands in the entrance tube to the static water level of the saturation container. The disadvantage of this method is that the sand may expand without one being able to visually determine this. A simple computation indicates that, if the sand in the mold expands, say, 0.40 cm, which is a distinct possibility, the change in the void ratio of the soil for G = 2.65 and $\gamma = 1.65$ gram/cm^3 is approximately as follows:

Sponsored by Committee on Subsurface Drainage.

Area of mold = $0.7854(10.16)^2 = 81.1$ cm^2,
Volume = $81.1(11.6) = 940.8$ cm^3,
$\Delta V = 81.1(0.40) = 32.4$ cm^3, and
Change in void ratio = 9.0 percent

Since it has been found that $k = f(e^2)$, this value can represent a considerable error in k. The soil expansion and saturation problems are avoided in the ASTM test D2434-68 via use of a plastic cylinder having a spring that confines the soil specimen. The ASTM apparatus is rather complicated, however, compared to the device used by the author in the series of tests described here.

APPARATUS AND PRELIMINARY PROCEDURE

To obtain valid results for comparison, it was necessary to first modify the standard compaction permeability device to avoid sample drainage. This was done by installing an exit gooseneck as shown in Figure 1. The gooseneck could be used as a telltale for the degree of sample saturation; i.e., when the inlet source is clamped, the exit flow immediately halts if the sample is saturated; otherwise, flow continues until the entrapped air expands to equilibrium pressure.

The standard commercially available permeability device has a rather small inlet orifice, which was not modified. It was evident early in the testing that this was probably a factor of some importance; however, to determine the exact effect would require a complete redesign of the permeameter cover. The redesign would have to include an orifice enlargement as well as provide a means of diffusing the water so that the full force of the entering stream of water does not strike the soil at a single point as allowed in the present device. The ASTM device also has a problem of diffusing the entering water when a wire screen is used rather than a porous stone.

Because the standard device is already constructed and in use, it was the primary objective of this study to determine if the device was satisfactory as built. If the device was unsatisfactory compared to the author's device, what kind of error could one reasonably expect, could these be reduced, and what are the probable causes?

In earlier work, the author had noted that one could put water in an empty metal compaction permeameter with a time lag noted before the water flowed into the exit tube. The first step, therefore, was to determine the coefficient of permeability of the 1.3-cm thick porous stones. This was done for both sides of several stones when the stones had been used enough to have one side impregnated with fines. Table 1 gives the results. At this point, the author was aware that one might debate the validity of Darcy's law ($v = ki$) because these flow rates could be nonlaminar. On the other hand, as the flow rates are to be compared, it did not seem unreasonable to use the Darcy equation for the computations.

Table 1 indicates that the effect of the porous stone is a significant parameter when using these devices or any device using a porous stone including the ASTM-recommended permeameter configuration. The coefficient of permeability of the standard compaction mold without any porous stone was 347×10^{-3} cm/sec. The value is indicative of the rate of water flow through the mold and indicates that the entrance orifice provides a significant constriction or resistance to flow.

The plastic device developed by the author is shown in Figure 3. This device uses a No. 200 mesh screen top and bottom to confine the sample. A diffuser is used in the base to break up the entrance flow of water. This ensures that the flow is relatively uniform and of negligible entrance velocity across the base of the sample. Parts are machined such that flow restrictions are a minimum. The tail water is fixed such that the sample cannot possibly drain—through use of a large-diameter circular overflow weir. The exit tube is relatively large in diameter so that it can accommodate large flow quantities. The system is constructed such that, when the base is watertight, the soil sample cannot expand. Provision is also incorporated to put a vacuum on the sample. In spite of the fact that the sample uses a No. 200 mesh screen, the device is rugged enough so that, with reasonable care, one can build samples to almost any density

that is possible with the metal mold. If the screen becomes torn, it is relatively simple to cut and glue (epoxy) a new screen in place.

TESTING

A series of tests was undertaken using both graded and ungraded materials. Very fine sand and gravel were eliminated because the primary effort was toward testing the two devices on materials in a size range that could be used as filter materials for underdrainage systems. The size ranges used represent many of the more common sand deposits found in nature.

To reduce human error as much as possible and to spot erratic results if there were any, the following were test criteria:

1. The same density (as closely as possible) was used for a given soil.
2. The same differential head was used; however, this resulted in a hydraulic gradient of i = h/L for the two molds—$i_{metal\ mold}$ = 178.5/11.6 = 15.4, and $i_{plastic\ mold}$ = 178.5/20.3 = 8.8.
3. At least three separate samples were built in each device, and at least three separate test runs were made. In most cases four test runs were made because little extra time was involved.
4. All k-values were reduced to k at 20 C for ease of comparison.
5. The time to obtain the flow quantity, Q, for a set of data was held constant as given in Table 2.
6. De-aired water (but not distilled) was used in all tests.
7. Saturation was obtained in the metal device by attaching the de-aired water source to the exit tube and applying a very small head to back the water up through the sample. If the gooseneck telltale indicated too much entrapped air, the sample was discarded. Saturation of the plastic device was done entirely by visual inspection.
8. Samples were oven-dried and carefully reblended with the source material to make the next test sample.

The results were remarkably consistent for each type of device. A typical set of data is given in Table 2.

Table 3 gives a summary of the testing program. The k-values shown are the average values for three tests. Figure 4 shows the sieve analyses of the soils used. The one-size soils given in Table 3 are the separated portions of a large sample of the coarse sand.

The author considered both the usual computational procedure and a procedure including the capability of the porous stone to give effectively a two-layer soil system. This required a computation (Appendix) as follows:

$$k_{soil} = \frac{L_{soil}}{\frac{L_{rs}}{k_{rs}} - \frac{L_{rock}}{k_{rock}}} \qquad (1)$$

where k_{soil} is the nominal computed coefficient of permeability of the soil and rock system. The derivation, identification of terms, and use of Eq. 1 are given in the Appendix.

The data given in Table 3 indicate the effect of applying Eq. 1 instead of the usual computation for k of

$$k = \frac{QL}{Aht} \qquad (2)$$

where L = soil sample length of 11.6 cm. This has a considerable effect on the computed coefficients of permeability of the soil. The values given in Table 3, identified as $k_{nominal}$ for the metal mold, are obtained by using Eq. 2.

Figure 1. Standard compaction mold permeameter.

Figure 2. Modifying density of granular materials.

Figure 3. Plastic mold device.

Device disassembled; note overflow weir with top screen and diffuser with bottom screen assembly.

Building a sample.

Device assembled and in operation.

Table 1. Coefficients of permeability of porous stones.

Stone Number	Side 1 Up (cm/sec × 10^{-3})	Side 1 Down (cm/sec × 10^{-3})
28	2.27	2.31
7	2.00	1.87
30	2.32	2.31
2	2.27	2.29

Table 2. Permeability data of fine sand-coarse sand mixture.

Device	Time (sec)	Flow Quantity (cm^3)	Temperature (deg C)
Plastic mold[a] (diameter of 7.6 cm and length of 20.3 cm)	100	745	22
	100	733	21.5
	100	729	21.5
	100	720	21.5
Metal mold[b] (diameter of 10.16 cm and length of 11.6 cm)	70	828	24.5
	70	821	24.5
	70	820	24.5
	70	829	24.5

[a] $k_{20} = 1.74 \times 10^{-2}$ cm/sec.

[b] $k_{20} = 8.49 \times 10^{-3}$ cm/sec.

Table 3. Summary of test data.

Material	Sieve Passing	Sieve Retained	$k_{nominal}$ Metal Mold[a] (cm/sec × 10^{-3})	k_{soil} Metal Mold[b] (cm/sec × 10^{-2})	k Plastic Mold (cm/sec × 10^{-2})	Ratio $k_{plastic}/k_{nominal}$	Ratio $k_{plastic}/k_{actual}$	Unit Weight of Soil[c] (gram/cm^3)
Fine sand	—	—	8.25	1.38	1.71	2.07	1.24	1.70
Coarse sand	—	—	7.85	1.28	3.50	4.46	2.73	1.82
	No. 50	No. 100	3.57	0.433	0.875	2.45	2.03	1.57
	No. 30	No. 50	11.0	2.37	5.85	5.32	2.47	1.62
	No. 20	No. 30	11.1	2.39	7.26	6.54	3.03	1.60
	No. 10	No. 30	13.3	3.80	9.59	6.98	2.52	1.58
	No. 4	No. 10	14.4	4.70	1.33	4.94	2.74	1.78
Coarse sand with sand passing No. 60 sieve removed	—	—	11.4	2.05	5.63	4.94	2.74	1.78
50 percent fine sand and 50 percent coarse sand[d]	—	—	8.15	1.35	1.74	2.13	1.28	1.77

[a]Using Eq. 2 with L = 11.6 cm (usual method of computation).
[b]Using Eq. 1.
[c]Metal and plastic molds used same density.
[d]Average values shown include values from Table 2.

Figure 4. Sieve analysis of soils used.

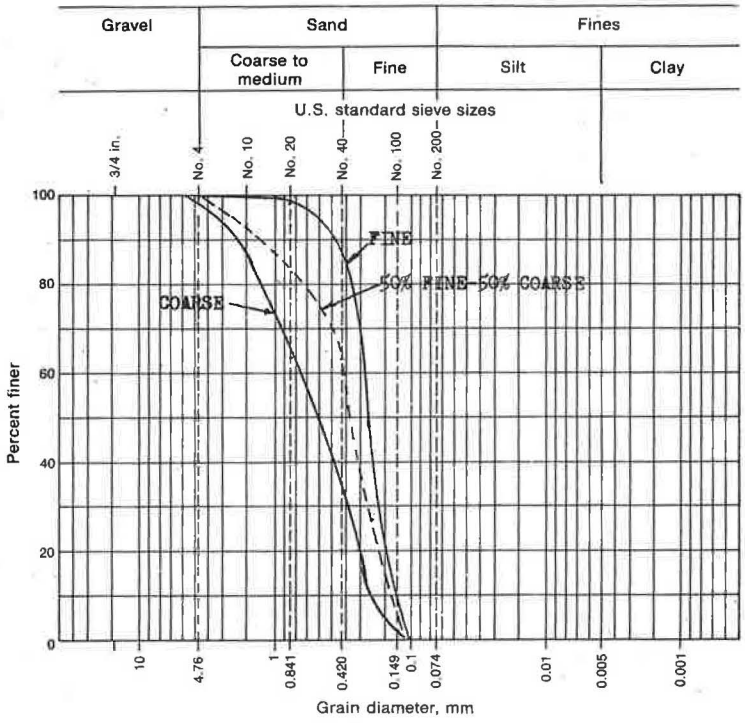

HIGHWAY RESEARCH RECORD 431

Page 59, in Table 3, following the "Coarse sand" entry, the 5th and 6th lines should read:

No. 10	No. 30	13.3	3.80	9.59	7.21	2.52	1.58
No. 4	No. 10	14.4	4.70	13.3	9.23	2.82	1.78

CONCLUSIONS

From the data given in Table 3, it appears that one should use permeability data from the compaction mold with caution. This device seems to give values of coefficient of permeability on the order of 2 to 9 times too small. The analysis given here indicates that the error can be reduced to about a factor of two if the metal mold is considered as a two-layer soil system. To use the two-layer soil system requires slight modification of the mold (the gooseneck) and determination of the k of the porous stone. Table 3 also indicates that, as the soil sample becomes finer (appreciable material smaller than the No. 100 sieve), the effect of the porous stone on the computed value of k decreases, which is in agreement with Eq. 1.

The discrepancy factor of two between the coefficients of permeability determined by using the plastic and the metal molds, after correcting the metal mold data as a two-layer system, is probably due to the small entrance orifice of the metal mold.

Use of the plastic device proved to be superior to the metal mold because of the following characteristics:

1. A two-layer computation is not needed;
2. Saturation is facilitated;
3. Soil expansion is not a problem;
4. If material segregation occurs, it can be visually observed and the sample rebuilt if necessary; and
5. Tail water control is not a problem.

It might be pointed out also that, in the use of the plastic device, the application of a vacuum to saturate a sample can actually produce the opposite effect. This is because any vacuum that is larger than the vapor pressure of water will vaporize the water (even de-aired water) when the water inlet is opened, producing an air (water vapor) bubble at the base of the soil sample. The author was never able to remove these bubbles when they formed and finally abandoned the use of a vacuum and instead very carefully controlled the inlet flow with periodic vacuum application to the water in the soil. He then reopened the exit tube so that the vacuum was returned to atmospheric pressure prior to adding more water. This process was repeated as deemed necessary until the water was level with the overflow weir.

REFERENCES

1. Bowles, J. E. Engineering Properties of Soils and Their Measurements. McGraw-Hill Book Co., 1970.
2. Burmister, D. M. Principles of Permeability Testing of Soils. Symposium on Permeability of Soils, ASTM, STP 163, 1954, pp. 3-26.
3. Chu, T. Y., Davidson, D. T., and Wickstrom, A. E. Permeability Test for Sands. Symposium on Permeability of Soils, ASTM, STP 163, 1954, pp. 43-55.
4. Yemington, E. G. A Low-Head Permeameter for Testing Granular Materials. Symposium on Permeability of Soils, ASTM, STP 163, 1954, pp. 37-42.

APPENDIX

DERIVATION AND USE OF EQUATION 1

The following steps are used to derive and use Eq. 1:

1. Compute the apparent coefficient of permeability of the soil ($k_{nominal}$) using Eq. 2

$$k = QL/Aht$$

Here L is the metal mold height of 11.6 cm. Using data from Table 2 as an example, we can consider the following: average Q = 824.5 cm and is collected in 70 sec at a

test of T = 24.5 C. The area of the standard compaction mold used in the test is 81.1 cm^2. Substituting these values gives

$$k_{24.5\,C} = 824.5(11.6)/81.1(178.5)(70) = 9.45 \times 10^{-3} \text{ cm/sec}$$

$$k_{20\,C} = 0.901(9.45 \times 10^{-3}) = 8.49 \times 10^{-3} \text{ cm/sec}$$

The average k_{20} value for the three tests on this material is 8.15×10^{-3} cm/sec as given in Table 3.

2. Vertical flow through a two-layer soil mass using the continuity of flow concept (saturation = 100 percent) is

$$\frac{L_{total}}{k_{equivalent}} = \frac{L_1}{k_1} + \frac{L_2}{k_2}$$

And for the soil-porous stone system this becomes

$$\frac{L_{rs}}{k_{rs}} = \frac{L_{soil}}{k_{soil}} + \frac{L_{rock}}{k_{rock}}$$

Because k_{soil} is desired, rearranging yields

$$k_{soil} = \frac{L_{soil}}{\frac{L_{rs}}{k_{rs}} - \frac{L_{rock}}{k_{rock}}} \qquad (1)$$

Values to use in Eq. 1 are L_{soil} = 11.6 cm and L_{rs} = 12.9 cm (rs = rock + soil); the values of L_{rock}/k_{rock} are given in Table 1. One may compute the values of k_{rs} as proportional to the thickness L_{rs} using the computed values of $k_{nominal}$. Thus,

$$k_{rs} = \frac{12.9}{11.6} k_{nominal}$$

Using the 50 percent fine-50 percent coarse sand value of $k_{nominal}$ from Table 3 and the No. 28 stone data from Table 1 of 2.3×10^{-3} cm/sec, the following are computed:

$$L_{rs}/k_{rs} = 12.9(11.6)/12.9(8.15 \times 10^{-3}) = 1{,}425$$

$$L_{rock}/k_{rock} = 1.3/(2.3 \times 10^{-3}) = 565$$

Substituting into Eq. 1

$$k_{soil} = 11.6/(1{,}425 - 565) = 1.35 \times 10^{-3} \text{ cm/sec}$$

Other entries in Table 3 are computed in a similar manner.

SPONSORSHIP OF THIS RECORD

GROUP 2—DESIGN AND CONSTRUCTION OF TRANSPORTATION FACILITIES
John L. Beaton, California Division of Highways, chairman

SOIL MECHANICS SECTION
Carl L. Monismith, University of California, Berkeley, chairman

Committee on Strength and Deformation Characteristics of Pavement Sections
John A. Deacon, University of Kentucky, chairman
Richard D. Barksdale, Bert E. Colley, Hsai-Yang Fang, F. N. Finn, Frank L. Holman, W. Ronald Hudson, Melvin H. Johnson, Bernard F. Kallas, William J. Kenis, Wolfgang G. Knauss, Milan Krukar, H. Gordon Larew, Fred Moavenzadeh, Carl L. Monismith, William M. Moore, Keshavan Nair, Eugene L. Skok, Jr., Ronald L. Terrel

Committee on Subsurface Drainage
Glen L. Martin, Montana State University, chairman
Reginald A. Barron, Mike Bealey, Paul J. Brudy, Harry R. Cedergren, Hsai-Yang Fang, Kenneth F. Ferrari, David S. Gedney, John G. Hendrickson, Jr., W. R. Lovering, Alfred W. Maner, Lyndon H. Moore, William B. Nern, Carl I. Olsen, T. W. Smith, W. T. Spencer, R. S. Standley

John W. Guinnee, Highway Research Board staff

The sponsoring committee is identified by a footnote on the first page of each report.